



**HAL**  
open science

## Widespread deoxygenation of temperate lakes

Stephen Jane, Gretchen Hansen, Benjamin Kraemer, Peter Leavitt, Joshua Mincer, Rebecca North, Rachel Pilla, Jonathan Stetler, Craig Williamson, R. Iestyn Woolway, et al.

► **To cite this version:**

Stephen Jane, Gretchen Hansen, Benjamin Kraemer, Peter Leavitt, Joshua Mincer, et al.. Widespread deoxygenation of temperate lakes. *Nature*, 2021, 594 (7861), pp.66-70. 10.1038/s41586-021-03550-y . hal-03303804

**HAL Id: hal-03303804**

**<https://hal.inrae.fr/hal-03303804v1>**

Submitted on 2 Jul 2024

**HAL** is a multi-disciplinary open access archive for the deposit and dissemination of scientific research documents, whether they are published or not. The documents may come from teaching and research institutions in France or abroad, or from public or private research centers.

L'archive ouverte pluridisciplinaire **HAL**, est destinée au dépôt et à la diffusion de documents scientifiques de niveau recherche, publiés ou non, émanant des établissements d'enseignement et de recherche français ou étrangers, des laboratoires publics ou privés.



Distributed under a Creative Commons Attribution 4.0 International License

# *Widespread deoxygenation of temperate lakes*

Article

Accepted Version

Jane, S. F., Hansen, G. J. A., Kraemer, B. M., Leavitt, P. R., Mincer, J. L., North, R. L., Pilla, R. M., Stetler, J. T., Williamson, C. E., Woolway, R. I. ORCID: <https://orcid.org/0000-0003-0498-7968>, Arvola, L., Chandra, S., DeGasperi, C. L., Diemer, L., Dunalska, J., Erina, O., Flaim, G., Grossart, H.-P., Hambright, K. D., Hein, C., Hejzlar, J., Janus, L. L., Jenny, J.-P., Jones, J. R., Knoll, L. B., Leoni, B., Mackay, E., Matsuzaki, S.-i. S., McBride, C., Müller-Navarra, D. C., Paterson, A. M., Pierson, D., Rogora, M., Rusak, J. A., Sadro, S., Saulnier-Talbot, E., Schmid, M., Sommaruga, R., Thiery, W., Verburg, P., Weathers, K. C., Weyhenmeyer, G. A., Yokota, K. and Rose, K. C. (2021) Widespread deoxygenation of temperate lakes. *Nature*, 594. pp. 66-70. ISSN 0028-0836 doi: <https://doi.org/10.1038/s41586-021-03550-y> Available at <https://centaur.reading.ac.uk/100084/>

It is advisable to refer to the publisher's version if you intend to cite from the work. See [Guidance on citing](#).

To link to this article DOI: <http://dx.doi.org/10.1038/s41586-021-03550-y>

Publisher: Nature Publishing Group

All outputs in CentAUR are protected by Intellectual Property Rights law, including copyright law. Copyright and IPR is retained by the creators or other copyright holders. Terms and conditions for use of this material are defined in the [End User Agreement](#).

[www.reading.ac.uk/centaur](http://www.reading.ac.uk/centaur)

## **CentAUR**

Central Archive at the University of Reading

Reading's research outputs online

1 **Title:**

2 Widespread deoxygenation of temperate lakes

3

4 **Authors:**

5 Stephen F. Jane<sup>1,2</sup>, Gretchen J. A. Hansen<sup>3</sup>, Benjamin M. Kraemer<sup>4</sup>, Peter R. Leavitt<sup>5,6</sup>, Joshua L.  
6 Mincer<sup>1</sup>, Rebecca L. North<sup>7</sup>, Rachel M. Pilla<sup>8</sup>, Jonathan T. Stetler<sup>1</sup>, Craig E. Williamson<sup>8</sup>, R.  
7 Iestyn Woolway<sup>9</sup>, Lauri Arvola<sup>10</sup>, Sudeep Chandra<sup>11</sup>, Curtis L. DeGasperis<sup>12</sup>, Laura Diemer<sup>13</sup>,  
8 Julita Dunalska<sup>14</sup>, Oxana Erina<sup>15</sup>, Giovanna Flaim<sup>16</sup>, Hans-Peter Grossart<sup>17, 18</sup>, K. David  
9 Hambright<sup>19</sup>, Catherine Hein<sup>20</sup>, Josef Hejzlar<sup>21</sup>, Lorraine L. Janus<sup>22</sup>, Jean-Philippe Jenny<sup>23</sup>, John  
10 R. Jones<sup>7</sup>, Lesley B. Knoll<sup>24</sup>, Barbara Leoni<sup>25</sup>, Eleanor Mackay<sup>26</sup>, Shin-Ichiro S. Matsuzaki<sup>27</sup>,  
11 Chris McBride<sup>28</sup>, Dörthe C. Müller-Navarra<sup>29</sup>, Andrew M. Paterson<sup>30</sup>, Don Pierson<sup>2</sup>, Michela  
12 Rogora<sup>31</sup>, James A. Rusak<sup>29</sup>, Steven Sadro<sup>32</sup>, Emilie Saulnier-Talbot<sup>33</sup>, Martin Schmid<sup>34</sup>, Ruben  
13 Sommaruga<sup>35</sup>, Wim Thiery<sup>36, 37</sup>, Piet Verburg<sup>38</sup>, Kathleen C. Weathers<sup>39</sup>, Gesa A.  
14 Weyhenmeyer<sup>2</sup>, Kiyoko Yokota<sup>40</sup>, and Kevin C. Rose<sup>1</sup>

15

16 1. Department of Biological Sciences, Rensselaer Polytechnic Institute, Troy, NY, USA

17 2. Department of Ecology and Genetics/Limnology, Uppsala University, Uppsala, Sweden

18 3. Department of Fisheries, Wildlife and Conservation Biology, University of Minnesota,  
19 St. Paul, MN, USA

20 4. Department of Ecosystem Research, IGB Leibniz institute for freshwater ecology and  
21 inland fisheries, Berlin, Germany

- 22 5. Institute of Environmental Change and Society, University of Regina, Regina,  
23 Saskatchewan, Canada
- 24 6. Institute for Global Food Security, Queen's University Belfast, Belfast, County Antrim,  
25 United Kingdom
- 26 7. School of Natural Resources, University of Missouri, Columbia, MO, USA
- 27 8. Department of Biology, Miami University, Oxford, OH, USA
- 28 9. Centre for Freshwater and Environmental Studies, Dundalk Institute of Technology,  
29 Dundalk, Ireland
- 30 10. Lammi Biological Station, University of Helsinki, Pääjärventie 320, Lammi, Finland
- 31 11. Biology Department and Global Water Center, University of Nevada, Reno, NV, USA
- 32 12. King County Water and Land Resources Division, Seattle, WA, USA
- 33 13. FB Environmental Associates, Portsmouth, NH, USA
- 34 14. Department of Water Protection Engineering, University of Warmia and Mazury in  
35 Olsztyn, Prawocheńskiego str. 1, Olsztyn, Poland
- 36 15. Department of Hydrology, Lomonosov Moscow State University, Leninskiye Gory 1,  
37 Moscow, Russia
- 38 16. Department of Sustainable Agro-ecosystems and Bioresources, Research and Innovation  
39 Centre, Fondazione Edmund Mach, San Michele all'Adige, Italy
- 40 17. Department of Experimental Limnology, Leibniz-Institute of Freshwater Ecology and  
41 Inland Fisheries, Alte Fischerhuetten 2, Stechlin, Germany

- 42 18. Institute of Biochemistry and Biology, Potsdam University, Maulbeerallee 2, Potsdam,  
43 Germany
- 44 19. Plankton Ecology and Limnology Laboratory, Geographical Ecology Group, and  
45 Program in Ecology and Evolutionary Biology, Department of Biology, The University  
46 of Oklahoma, Norman, Oklahoma, USA
- 47 20. Wisconsin Department of Natural Resources, Madison, WI, USA
- 48 21. Institute of Hydrobiology, Biology Centre CAS, Na Sádkách 7, České Budějovice, Czech  
49 Republic
- 50 22. Bureau of Water Supply, New York City Department of Environmental Protection, 465  
51 Columbus Ave., Valhalla, NY, USA
- 52 23. CARRTEL Limnology Center, Institut National de la Recherche Agronomique (INRA),  
53 Université Savoie Mont Blanc, 73000 Chambéry, France
- 54 24. Itasca Biological Station and Laboratories, University of Minnesota, Lake Itasca, MN,  
55 USA
- 56 25. Department of Earth and Environmental Sciences, University of Milan-Bicocca, Piazza  
57 della Scienza 1, Milan, Italy
- 58 26. Lake Ecosystems Group, Centre for Ecology & Hydrology, Bailrigg, Lancaster, United  
59 Kingdom
- 60 27. Center for Environmental Biology and Ecosystem Studies, National Institute for  
61 Environmental Studies, 16-2 Tsukuba, Ibaraki, Japan
- 62 28. Environmental Research Institute, Hamilton, New Zealand

- 63 29. Department of Biology, University of Hamburg, Hamburg, Germany
- 64 30. Ontario Ministry of the Environment, Conservation and Parks, Dorset Environmental  
65 Science Centre, Dorset, ON, Canada
- 66 31. CNR Water Research Institute, L. go Tonolli 50, Verbania Pallanza, Italy
- 67 32. Department of Environmental Science and Policy, University of California, One Shields  
68 Ave., Davis, CA, USA
- 69 33. Centre d'études nordiques (CEN) and Faculty of Sciences and Engineering, Université  
70 Laval, Québec, Canada
- 71 34. Eawag, Swiss Federal Institute of Aquatic Science and Technology, Surface Waters –  
72 Research and Management, Kastanienbaum, Switzerland
- 73 35. Department of Ecology, University of Innsbruck, Innsbruck, Austria
- 74 36. Vrije Universiteit Brussel, Department of Hydrology and Hydraulic Engineering,  
75 Pleinlaan 2, Brussels, Belgium
- 76 37. ETH Zurich, Institute for Atmospheric and Climate Science, Universitaetstrasse 16,  
77 Zurich, Switzerland
- 78 38. National Institute of Water and Atmospheric Research Ltd (NIWA), Gate 10 Silverdale  
79 Rd., Hillcrest, Hamilton, New Zealand
- 80 39. Cary Institute of Ecosystem Studies, Box AB, Millbrook, New York, USA
- 81 40. Biology Department, State University of New York College at Oneonta (SUNY  
82 Oneonta), Oneonta, New York, USA

83 **Summary paragraph:**

84 The concentration of dissolved oxygen in aquatic systems helps regulate biodiversity<sup>1, 2</sup>, nutrient  
85 biogeochemistry<sup>3</sup>, greenhouse gas emissions<sup>4</sup>, and drinking water quality<sup>5</sup>. The long-term  
86 declines in dissolved oxygen concentrations in coastal and ocean waters have been linked to  
87 climate warming and human activity<sup>6, 7</sup>, but little is known about changes in dissolved oxygen  
88 concentrations in lakes. While dissolved oxygen solubility decreases with increasing water  
89 temperatures, long-term lake trajectories are not necessarily predictable. Oxygen losses in  
90 warming lakes may be amplified by enhanced decomposition and stronger thermal stratification<sup>8</sup>,  
91 <sup>9</sup> or they may increase as a result of enhanced primary production<sup>10</sup>. Here we analyse 45,148  
92 dissolved oxygen and temperature profiles from 393 temperate lakes spanning 1941-2017. We  
93 find that a decline in dissolved oxygen is widespread in surface and deep-water habitats. The  
94 decline in surface waters is primarily associated with reduced solubility under warmer water  
95 temperatures, although surface dissolved oxygen increased in a subset of highly-productive  
96 warming lakes, likely due to increasing phytoplankton production. In contrast, the decline in  
97 deep waters is associated with stronger thermal stratification and water clarity losses, but not  
98 with changes in gas solubility. Our results suggest that climate change and declining water  
99 clarity have altered the physical and chemical environment of lakes. Freshwater dissolved  
100 oxygen losses are 2.5-10 times greater than observed in the world's oceans<sup>6, 7</sup> and could threaten  
101 essential lake ecosystem services<sup>2, 3, 5, 11</sup>.

102

103

104



105 **Main text:**

106 The concentration of dissolved oxygen (DO) in aquatic systems influences biodiversity<sup>1</sup>,  
107 <sup>2</sup>, nutrient biogeochemistry<sup>3</sup>, greenhouse gas emissions<sup>4</sup>, drinking water quality<sup>5</sup>, and, ultimately,  
108 human health<sup>12</sup>. Many aquatic species require well-oxygenated habitat<sup>11, 13</sup> and cool water to  
109 survive warm summers<sup>2, 11</sup>. Loss of deep-water DO degrades water quality by promoting the  
110 release of accumulated nutrients from sediments into water<sup>1, 3</sup>, which can increase phytoplankton  
111 biomass. This process can also facilitate harmful algal blooms<sup>5</sup>, which can compromise water  
112 supplies and harm human health<sup>12</sup>. Despite clear evidence of large-scale deoxygenation in ocean  
113 waters<sup>6, 7</sup>, there are no systematic large-scale studies of this phenomenon in lakes<sup>3</sup>.

114 DO concentrations should decline with increasing water temperature due to reduced gas  
115 solubility. However, other mechanisms can alter DO, potentially amplifying or counteracting  
116 losses predicted from solubility changes alone. For example, rates of heterotrophic respiration  
117 increase with temperature faster than primary production<sup>9</sup>, and surface-temperature warming can  
118 increase the strength and duration of thermal stratification, reducing water circulation, and  
119 preventing deep-water DO replenishment<sup>8, 14, 15</sup>. Studies of individual lakes demonstrate deep-  
120 water DO concentrations can decrease with lake warming<sup>3, 8, 15, 16</sup>, reducing access to cold-water  
121 habitat essential to many organisms<sup>11</sup>. However, given the many feedbacks and processes  
122 regulating DO, overall trajectories currently defy *a priori* prediction.

123 We addressed this critical issue by compiling and analyzing an extensive database of lake  
124 temperature and DO profiles to characterize widespread and long-term changes in DO  
125 concentration and its causes. We used data from 393 temperate lake and reservoir basins, each  
126 with a minimum of 15 years of observation (median: 24 years), and report population medians  
127 from long-term surface- (epilimnion) and deep-water (hypolimnion) trends in temperature, DO

128 concentration, and DO saturation during the late summer period when seasonal DO depletion is  
129 expected to be pronounced<sup>17</sup>. Our analyses revealed that lake DO concentrations have declined in  
130 both surface and deep waters from 1980 to 2017 by 0.45 and 0.42 mg L<sup>-1</sup>, respectively (Fig. 1).  
131 These rates represent losses of 5.1 and 20.2% for surface and deep waters, respectively, and were  
132 substantially greater than those observed for the oceans, where total water-column DO has  
133 declined about 2% since 1960<sup>6</sup>.

134 While deep-water temperatures have been virtually stable since observations began (Fig.  
135 1a;  $-0.01^{\circ}\text{C decade}^{-1}$ ), both deep-water DO concentration and percent saturation declined  
136 through time ( $-0.12 \text{ mg L}^{-1} \text{ decade}^{-1}$  and  $-1.2\% \text{ decade}^{-1}$ ; respectively, Fig. 1b, c). Declines were  
137 unrelated to solubility as predicted changes based on solubility (slight increase of  $0.01 \text{ mg L}^{-1}$ )  
138 were negligible compared with observed losses (median  $-0.23 \text{ mg L}^{-1}$  based on last five years  
139 relative to first five years of each time series, Fig. 2b) Declining DO, despite essentially  
140 unchanging solubility, implies deep-water habitats have become increasingly inhospitable for  
141 organisms with aerobic metabolism, including fishes. We quantified potential impacts of such  
142 declines on habitat availability by calculating trends in  $T_{\text{DO}3}$ , the minimum water column  
143 temperature where DO was at least  $3 \text{ mg L}^{-1}$ . This metric was developed to quantify oxy-thermal  
144 habitats for cold-water fisheries<sup>11</sup>. In lakes where DO was below  $3 \text{ mg L}^{-1}$  anywhere in the water  
145 column at least once in the time series ( $n = 369$ ),  $T_{\text{DO}3}$  increased by  $0.17^{\circ}\text{C decade}^{-1}$ , with 68.0%  
146 of lakes having positive trends and declining habitat for many cold-water species.

147 In contrast to trends observed for deep waters, variation in surface-water DO  
148 concentrations was well explained by changes in gas solubility. Consistent with other global-  
149 scale lake studies<sup>18</sup>, median air temperatures warmed at  $0.30^{\circ}\text{C decade}^{-1}$  and median lake surface  
150 waters warmed at  $0.39^{\circ}\text{C decade}^{-1}$ . Additionally, median wind speed and precipitation declined

151 (trends of  $-0.04 \text{ m s}^{-1} \text{ decade}^{-1}$  and  $-4.23 \text{ mm decade}^{-1}$ , respectively), while shortwave radiation  
152 increased ( $1.88 \text{ W m}^2 \text{ decade}^{-1}$ ; Table S1). Surface-water temperature increases were best  
153 explained by spring and summer air temperature increases and by summer wind speed declines  
154 (Table S2). Surface-water DO concentrations declined at  $-0.11 \text{ mg L}^{-1} \text{ decade}^{-1}$  (Fig. 1b).  
155 Comparing the last five years relative to first five years of each time series revealed that the  
156 median change predicted due to solubility loss was  $\sim 63\%$  of the median observed decline in DO  
157 concentration, with solubility-predicted loss of  $0.12$  versus observed losses of  $0.19 \text{ mg L}^{-1}$  (Fig.  
158 2a).

159         Despite a strong influence of water temperature on DO concentration in surface-waters,  
160 there was substantial variability among lakes (Fig. 2a), and a large subset of lakes exhibited  
161 increases in both water temperature and DO concentration ( $n=87$ ; Fig. 3d). Analysis of the  
162 interaction between DO concentration, surface temperature, and water clarity (measured as  
163 Secchi depth, a proxy for trophic status<sup>19</sup>) showed that DO concentration generally decreased  
164 with increasing temperature. However, in lakes with low water clarity ( $< 2 \text{ m}$ ), DO concentration  
165 increased when average mean summer surface-water temperatures exceeded  $\sim 24^\circ\text{C}$  (Fig. 3c).  
166 Similarly, in a subset of lakes with chlorophyll data (a proxy for phytoplankton biomass;  $n =$   
167 162), positive DO trends were observed when chlorophyll was high and surface temperatures  
168 exceeded  $\sim 25^\circ\text{C}$ , (Fig. 3b;  $P < 0.001$ ). Thus, we suggest that eutrophication and warming interact  
169 to increase surface-water DO concentration despite reduced gas solubility.

170         Lakes with increasing DO concentration in warming surface waters had significantly  
171 higher surface-water temperatures (Fig. 3a;  $P = 0.016$ ) and their watersheds contained a  
172 significantly higher proportion of agriculture ( $P = 0.046$ ) and developed land cover ( $P < 0.001$ )  
173 compared with other lakes. When developed land exceeded  $\sim 50\%$  of a watershed and surface

174 water temperature exceeded  $\sim 25^{\circ}\text{C}$ , the probability of a warming lake having an increasing DO  
175 trend was  $>50\%$ . Combined, these analyses highlight a potential threshold above which water  
176 temperatures and lake productivity interact to elevate DO concentration in surface waters despite  
177 declining gas solubility. While we lack data on phytoplankton taxonomic composition, evidence  
178 indicates that phytoplankton blooms are increasing globally<sup>20</sup>, in particular due to  
179 cyanobacteria<sup>21</sup>. High temperatures and elevated nutrient loading can promote surface  
180 cyanobacteria blooms whose photosynthesis leads to DO supersaturation, particularly in  
181 eutrophic lakes as temperatures exceed  $\sim 23\text{-}25^{\circ}\text{C}$ <sup>10, 21</sup>. Consistent with this inferred mechanism,  
182 we note these same lakes exhibited consistently low deep-water DO concentration (median:  $0.64$   
183  $\text{mg L}^{-1}$ ) relative to other lakes (median:  $3.42 \text{ mg L}^{-1}$ ), as is expected when a large phytoplankton  
184 biomass sinks and is decomposed in deep-water habitats<sup>22</sup>. Deep water DO changes are described  
185 in more detail below.

186         Decadal-scale trends in DO were associated with non-linear changes in surface-water  
187 temperature (Fig. 2c-f; Fig. S1). For example, although surface-water temperatures generally  
188 increased from 1980 onwards, there was a period of accelerated increase during 1990-2000, with  
189 slower warming thereafter (Fig. 2c), consistent with the “warming hiatus” observed during 1998-  
190 2012<sup>23</sup>. This trend occurs across the population of all lakes, as well as the subset of lakes  
191 sampled continuously throughout this period. Similarly, surface-water DO exhibited periodic  
192 deviations from an overarching trend of declining DO concentration (Fig. 2d), mainly due to the  
193 productive lakes exhibiting increasing DO levels in surface waters (Fig. 2d, blue line). Excluding  
194 these lakes, analysis of the remaining sites showed a consistent long-term decline in surface-  
195 water DO (Fig. 2d, red line). Deep-water temperatures exhibited a pronounced multi-decadal

196 oscillation since 1980 (Fig. 2e) as has been observed in some lakes previously<sup>24</sup>, whereas deep-  
197 water DO concentration declined consistently through time (Fig. 2f).

198         While surface-water DO concentration changes were generally well predicted by  
199 solubility changes, deep-water DO changes were more strongly associated with changes in water  
200 clarity and water-column density differences (Figs. 4 and S2). For example, water clarity losses  
201 exceeding 1 m were associated with substantial reductions in deep-water DO saturation (Fig.  
202 S2). Mechanistically, increases in phytoplankton biomass or dissolved organic matter (DOM)  
203 reduce water clarity while increasing oxygen-consuming respiration<sup>19, 22, 25</sup>. Increases in  
204 phytoplankton biomass and DOM are often caused by land use change and recovery from acid  
205 deposition, respectively<sup>26</sup>. However, there was no overarching decline in water clarity across  
206 study lakes. Indeed, 51% of lakes had clarity increases and 49% had decreases, and only 39% of  
207 lakes exhibited both water clarity loss and DO saturation loss (Fig. 4a).

208         Deep-water DO decreased substantially in lakes where the water column density  
209 difference between surface and deep waters increased by more than  $\sim 0.5 \text{ kg m}^{-3}$  (Fig 4b; Fig.  
210 S2b). Strong increases in the density difference indicate intensified stratification that reduces  
211 vertical mixing and replenishment of deep-water DO from the atmosphere, and may reduce  
212 nutrient upwelling to surface waters<sup>3, 15</sup>. Water column density differences increase due to water  
213 clarity losses as well as other factors that increase heat gain in near-surface waters, including  
214 climate warming<sup>26</sup> and atmospheric stilling<sup>27</sup>. Increased water column density differences may  
215 also be associated with earlier onset of seasonal stratification and thus more time for oxygen  
216 consumption before the summer sampling period<sup>22</sup>. We found that changes in water-column  
217 density differences were best explained by changes in deep water temperature and climate  
218 characteristics (Fig. S3). Despite no overarching among-lake trend in water clarity or deep-water

219 temperature, stratification strength increased in 84% of lakes that stratified, with 61% of basins  
220 exhibiting both increased density difference and DO saturation loss (Fig 4b). Warming surface-  
221 water temperatures combined with unchanging deep-water temperatures (Fig. 1a) increases the  
222 density difference in lake water columns (median rate:  $0.10 \text{ kg m}^{-3} \text{ decade}^{-1}$ ). We observed  
223 unchanging deep-water DO in lakes where both clarity and stratification were unchanged (Fig.  
224 4c, d). Therefore, we anticipate further DO losses in deep waters of lakes where water clarity  
225 continues to decline or thermal stratification intensifies, whether due to atmospheric warming,  
226 stilling, or both<sup>26, 27</sup>.

227         Despite a wide range of lake and catchment characteristics, the overall trend of temperate  
228 lake deoxygenation is clear, with climate changes and water clarity losses contributing to  
229 declines in lake DO concentration at rates  $\sim 2.5$ -10 times greater than those observed in the global  
230 oceans<sup>6, 7</sup>. We find deep-water lake habitats are especially threatened, and deep-water DO trends  
231 may portend future losses of cold-water and oxygen-sensitive species<sup>2</sup>, increased internal  
232 nutrient loading which exacerbates eutrophication<sup>3</sup> and the formation of harmful algal blooms<sup>5</sup>,  
233 and potentially increased outgassing of stored methane<sup>4</sup>. While already rapid, future losses in  
234 lake DO may accelerate due to continued anthropogenic modifications of the environment,  
235 including eutrophication<sup>22</sup>, salinization<sup>28</sup>, and hydrological management<sup>28</sup>. While many lakes  
236 have undergone active management to reduce nutrient loads, in part to mitigate phytoplankton  
237 growth and deep-water oxygen loss<sup>28</sup>, our findings suggest such actions will likely require more  
238 rigorous efforts in the future to counter the effects of climate and land use change.

239

240 **References:**

- 241 1. Wetzel, R. G. 2001. Chap. 9 oxygen. In: *Limnology*, 3<sup>rd</sup> edn (ed Wetzel R. G.), pp 151-168,  
242 Academic Press, San Diego.
- 243 2. Schindler, D. Warmer climate squeezes aquatic predators out of their preferred habitat. *Proc.*  
244 *Natl. Acad. Sci.*, **114**, 9764-9765 (2017).
- 245 3. North, R. P., North, R. L., Livingstone, D. M., Köster, O., & Kipfer, R. Long-term changes  
246 in hypoxia and soluble reactive phosphorus in the hypolimnion of a large temperate lake:  
247 consequences of a climate regime shift. *Glob. Change Biol.*, **20**, 811-823 (2014).
- 248 4. Fernández, J. E., Peeters, F., & Hofmann, H. Importance of the autumn overturn and anoxic  
249 conditions in the hypolimnion for the annual methane emissions from a temperate lake.  
250 *Environ. Sci. Technol.*, **48**, 7297-7304 (2014).
- 251 5. Michalak, A. M., et al. Record-setting algal bloom in Lake Erie caused by agricultural and  
252 meteorological trends consistent with expected future conditions. *Proc. Natl. Acad. Sci.*, **110**,  
253 6448-6452 (2013).
- 254 6. Schmidtko, S., Stramma, L., & Visbeck, M. Decline in global oceanic oxygen content during  
255 the past five decades. *Nature*, **542**, 335-339 (2017).
- 256 7. Breitburg, D., et al. Declining oxygen in the global ocean and coastal waters. *Science*, **359**,  
257 DOI: 10.1126/science.aam7240 (2018).
- 258 8. Jankowski, J., Livingstone, D. M., Bührer, H., Forster, R., & Niederhauser, P. Consequences  
259 of the 2003 European heat wave for lake temperature profiles, thermal stability, and

- 260 hypolimnetic oxygen depletion: Implications for a warmer world. *Limnol. Oceanogr.*, **51**,  
261 815-819 (2006).
- 262 9. Yvon-Durocher, G., Jones, J. I., Trimmer, M., Woodward, G., & Montoya, J. M. Warming  
263 alters the metabolic balance of ecosystems. *Philos. T. R. Soc. B*, **365**, 2117-2126 (2010).
- 264 10. Seki, H., Takahashi, Y., Hara, Y., & Ichimura, S. Dynamics of dissolved oxygen during algal  
265 bloom in Lake Kasumigaura, Japan. *Water Res.*, **14**, 179-183 (1980).
- 266 11. Jacobson, P. C., Stefan, H. G., & Pereira, D. L. Coldwater fish oxythermal habitat in  
267 Minnesota lakes: influence of total phosphorus, July air temperature, and relative depth. *Can.*  
268 *J. Fish. Aquat. Sci.*, **67**, 2002-2013 (2010).
- 269 12. Harke, M. J., et al. A review of the global ecology, genomics, and biogeography of the toxic  
270 cyanobacterium, *Microcystis* spp. *Harmful Algae*, **54**, 4-20 (2016).
- 271 13. Vaquer-Sunyer, R., & Duarte, C. M. Thresholds of hypoxia for marine biodiversity. *Proc.*  
272 *Natl. Acad. Sci.*, **105**, 15452-15457 (2008).
- 273 14. Woolway, R. I., & Merchant, C. J. Worldwide alteration of lake mixing regimes in response  
274 to climate change. *Nat. Geosci.*, **12**, 271-276 (2019).
- 275 15. Livingstone, D. M. Impact of secular climate change on the thermal structure of a large  
276 temperate central European lake. *Clim. Change*, **57**, 205-225 (2003).
- 277 16. Zhang, Y., et al. Dissolved oxygen stratification and response to thermal structure and long-  
278 term climate change in a large and deep subtropical reservoir (Lake Qiandaohu, China).  
279 *Water Res.*, **75**, 249-258 (2015).



- 280 17. Bouffard, D., Ackerman, J. D., & Boegman, L. Factors affecting the development and  
281 dynamics of hypoxia in a large shallow stratified lake: hourly to seasonal patterns. *Water*  
282 *Resour. Res.*, **49**, 2380-2394 (2013).
- 283 18. O'Reilly, C. M., et al. Rapid and highly variable warming of lake surface waters around the  
284 globe. *Geophys. Res. Lett.*, **42**, 10773-10781 (2015).
- 285 19. Nürnberg, G. K. Trophic state of clear and colored, soft- and hardwater lakes with special  
286 consideration of nutrients, anoxia, phytoplankton and fish. *Lake Reserv. Manag.*, **12**, 432-447  
287 (1996).
- 288 20. Ho, J. C., Michalak, A. M., & Pahlevan, N. Widespread global increase in intense lake  
289 phytoplankton blooms since the 1980s. *Nature*, **574**, 667-670 (2019).
- 290 21. Kosten, S., et al. Warmer climates boost cyanobacterial dominance in shallow lakes. *Glob.*  
291 *Change Biol.*, **18**, 118-126 (2012).
- 292 22. Müller, B., Bryant, L. D., Matzinger, A., & Wüest, A. Hypolimnetic oxygen depletion in  
293 eutrophic lakes. *Environ. Sci. Technol.*, **46**, 9964-9971 (2012).
- 294 23. Winslow, L. A., Leach, T. A., & Rose, K. C. Global lake response to the recent warming  
295 hiatus. *Environ. Res. Lett.*, **13**, 054005 (2018).
- 296 24. Livingstone, D. M. An example of the simultaneous occurrence of climate-driven “sawtooth”  
297 deep-water warming/cooling episodes in several Swiss lakes, *Verh. Int. Ver. Limnol.*, **26**,  
298 822-828 (1997).
- 299 25. Williamson, C. E., et al. Ecological consequences of long-term browning in lakes. *Sci. Rep.*,  
300 **5**, DOI:10.1038/srep18666, (2015).

- 301 26. Rose, K. C., Winslow, L. A., Read, J. S., & Hansen, G. J. A. Climate-induced warming of  
302 lakes can be either amplified or suppressed by trends in water clarity. *Limnol. Oceanogr.*  
303 *Letters.*, **1**, 44-53 (2016).
- 304 27. Woolway, R. I., Merchant, C. J., Van Den Hoek, J., Azorin-Molina, C., Nöges, P., Laas, A.,  
305 Mackay, E. B., and Jones, I. D. Northern hemisphere atmospheric stilling accelerates lake  
306 thermal responses to a warming world. *Geophys. Res. Lett.*, **46**, 11983-11992 (2019).
- 307 28. Carpenter, S. R., Stanley, E. H., & Vander Zander, M. J. State of the world's freshwater  
308 ecosystems: physical, chemical, and biological changes. *Annu. Rev. Env. Resour.*, **36**, 75-99  
309 (2011).
- 310
- 311

312 **Acknowledgments:** This manuscript benefited from conversations at meetings of the Global  
313 Lake Ecological Observatory Network (GLEON; supported by funding from US NSF grants  
314 1137327 and 1702991). SFJ and KCR acknowledge support from US NSF grants 1638704,  
315 1754265, and 1761805 and SFJ was supported by a US Fulbright Student grant to Uppsala  
316 University, Sweden. GH acknowledges the many employees of the Minnesota Department of  
317 Natural Resources, the Minnesota Pollution Control agency, and citizen volunteers for data  
318 collection and collation. PRL acknowledges support from a NSERC Discovery Grant, the  
319 Canada Research Chair Program, Canada Foundation for Innovation, the Province of  
320 Saskatchewan, University of Regina, and Queen's University Belfast. RLN & JJ acknowledge  
321 support from the Missouri Department of Natural Resources and the Missouri Agricultural  
322 Experiment Station and many students that collected and processed reservoir samples under the  
323 leadership of Daniel V. Obrecht and Anthony P. Thorpe. RMP and CEW acknowledge support  
324 from NSF grants 1754276 and 1950170, Miami University Eminent Scholar Fund, and the  
325 Lacawac Sanctuary and Biological Field Station for access to Lake Lacawac and use of research  
326 facilities. RIW acknowledges support from the European Union's Horizon 2020 research and  
327 innovation programme under the Marie Skłodowska-Curie grant agreement No. 791812. SC  
328 acknowledges support of the Castle Lake Research Program through the University of Nevada  
329 and UC Davis via Charles R. Goldman. CLD acknowledges the King County Environmental  
330 Laboratory for the long-term monitoring data for Lake Washington and Lake Sammamish. JD  
331 acknowledges support from the University of Warmia and Mazury in Olsztyn (Grant under the  
332 Senate Committee for International Cooperation financing) and staff at Department of Water  
333 Protection Engineering for long-term data collection and analysis. OE acknowledges support  
334 from the Russian Scientific Foundation (grant 19-77-30004) for Mozhaysk Reservoir. GF

335 acknowledges support for long-term sampling of Lake Caldonazzo by the Fondazione Edmund  
336 Mach. HPG acknowledges funding for long-term sampling of Lake Stechlin by the Leibniz  
337 association and assistance by members of the IGB team. KDH acknowledges the Oklahoma  
338 Department of Wildlife Conservation, the Oklahoma Water Resources Board, the Grand River  
339 Dam Authority, the US Army Corps of Engineers, the City of Tulsa, W.M. Matthews, T. Clyde,  
340 R.M Zamor, P. Koenig, and R. West for support, assistance, and data for Lakes Texoma,  
341 Thunderbird, Grand, Eucha, and Spavinaw. JH acknowledges support from the ERDF/ESF  
342 project Biomanipulation as a tool for improving water quality of dam reservoirs (No  
343 CZ.02.1.01/0.0/0.0/16\_025/0007417). BL acknowledges support from the FA-UNIMIB for long-  
344 term monitoring of Lake Iseo. EBM acknowledges support from the UK Natural Environment  
345 Research Council funding for the long-term monitoring on Blelham Tarn and the staff of the  
346 Freshwater Biological Association and UK Centre for Ecology and Hydrology for carrying out  
347 the work. AP and JAR acknowledge support from the Ontario Ministry of the Environment,  
348 Conservation and Parks for providing data from south-central Ontario lakes (“Dorset lakes”) and  
349 staff and students at Ontario’s Dorset Environmental Science Centre for data collection and  
350 analysis. MR acknowledges the International Commission for the Protection of Italian-Swiss  
351 Waters (CIPAIS) for funding long-term research on Lake Maggiore. EST acknowledges Prof.  
352 Lauren Chapman (McGill University) and her team for the long-term data collection in Lake  
353 Nkuruba. MS acknowledges the City of Zurich Water Supply and the cantonal agencies of the  
354 cantons of Bern (AWA, Gewässer- und Bodenschutzlabor), Zurich (AWEL), St. Gallen (AFU),  
355 and Neuchatel for providing data for the Swiss lakes, CIPEL and INRA for data from Lake  
356 Geneva, and IGKB for data from Lake Constance. WT acknowledges support from the Belgian  
357 Science Policy Office through the research project EAGLES (CD/AR/02A) on Lake Kivu. PV

358 acknowledges support from the councils of the regions of Waikato, West Coast, and Bay of  
359 Plenty for long-term sampling of lakes Taupo, Brunner, and Tarawera. KY acknowledges  
360 support from the Clark Foundation for long-term monitoring of Otsego Lake and past and current  
361 members of SUNY Oneonta BFS for sampling. KS and JS acknowledge the National Park  
362 Service, W Gawley, Acadia National Park for providing data for Jordan Pond, Bubble Pond, and  
363 Eagle Lake in Maine. The views expressed in this article are those of the authors and do not  
364 necessarily reflect views or policies of funding agencies.

365

366 **Authorship contributions:** SFJ and KCR designed the study, compiled the data, conducted  
367 analyses, and drafted the manuscript. GJAH, BMK, PRL, JLM, RLN, RMP, JTS, CEW and RIW  
368 helped design the study and conduct analyses, contributed data, and edited the manuscript. All  
369 other authors contributed data, edited the manuscript, or both.

370

371 **Author information:** Derived statistics used in our analyses are publicly available via the  
372 Environmental Data Initiative (EDI) repository at:

373 <https://doi.org/10.6073/pasta/ac8b05bb0da19032b3df3efc21f83874>.

374 Reprints and permissions information is available at [www.nature.com/reprints](http://www.nature.com/reprints). The authors  
375 declare no competing interests.

376 Correspondence and requests for materials should be addressed to KCR ([rosek4@rpi.edu](mailto:rosek4@rpi.edu)).

377

378 **Figures and Figure Captions:**

379 **Fig. 1 | Trends in dissolved oxygen and temperature. a-c,** Density plots of trend magnitudes  
380 for **a** temperature ( $^{\circ}\text{C decade}^{-1}$ ), **b** DO concentration ( $\text{mg L}^{-1} \text{ decade}^{-1}$ ) and **c** DO percent  
381 saturation ( $\% \text{ decade}^{-1}$ ). Red distribution indicates surface water trends and blue indicates deep-  
382 water trends. The x-axis range for each plot covers two standard deviations from the median, or  
383 approximately 95% of data. Vertical dashed lines indicate median trends, and the zero trend is  
384 highlighted with a black vertical line.

385

386 **Fig. 2 | Solubility effects and changes in temperature and DO concentration through time.**  
387 **a, b,** Observed vs. predicted change in DO concentration ( $\text{mg L}^{-1}$ ) due to solubility for surface  
388 **(a)** and deep **(b)** waters. Solid black line is the 1:1 line and the blue line is loess smoothed, while  
389 the gray regions are 95% confidence intervals. **c-f,** Smoothed curves of GAMM models, showing  
390 deviation from the mean model predictions for selected response variables with year as the  
391 predictor variable. Gray regions represent one standard error from the predicted line for **c,**  
392 temperature ( $^{\circ}\text{C}$ ) and **d,** DO ( $\text{mg L}^{-1}$ ) through time for surface waters. The red line represents  
393 lakes where both surface temperature and DO were increasing ( $n = 87$ ) and the blue line is all  
394 other lakes ( $n = 332$ ). **e,** Temperature and **f,** DO for deep waters.

395

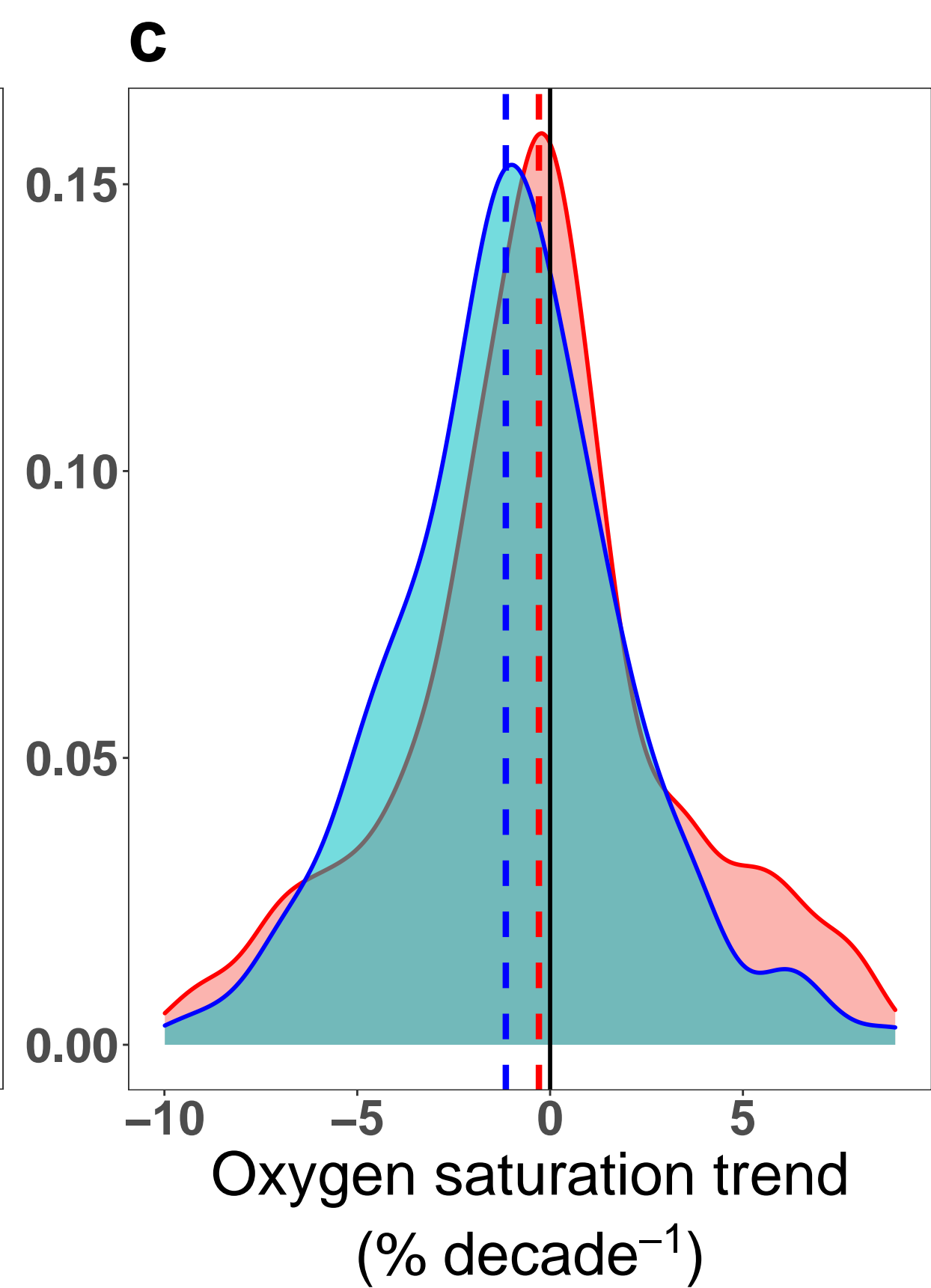
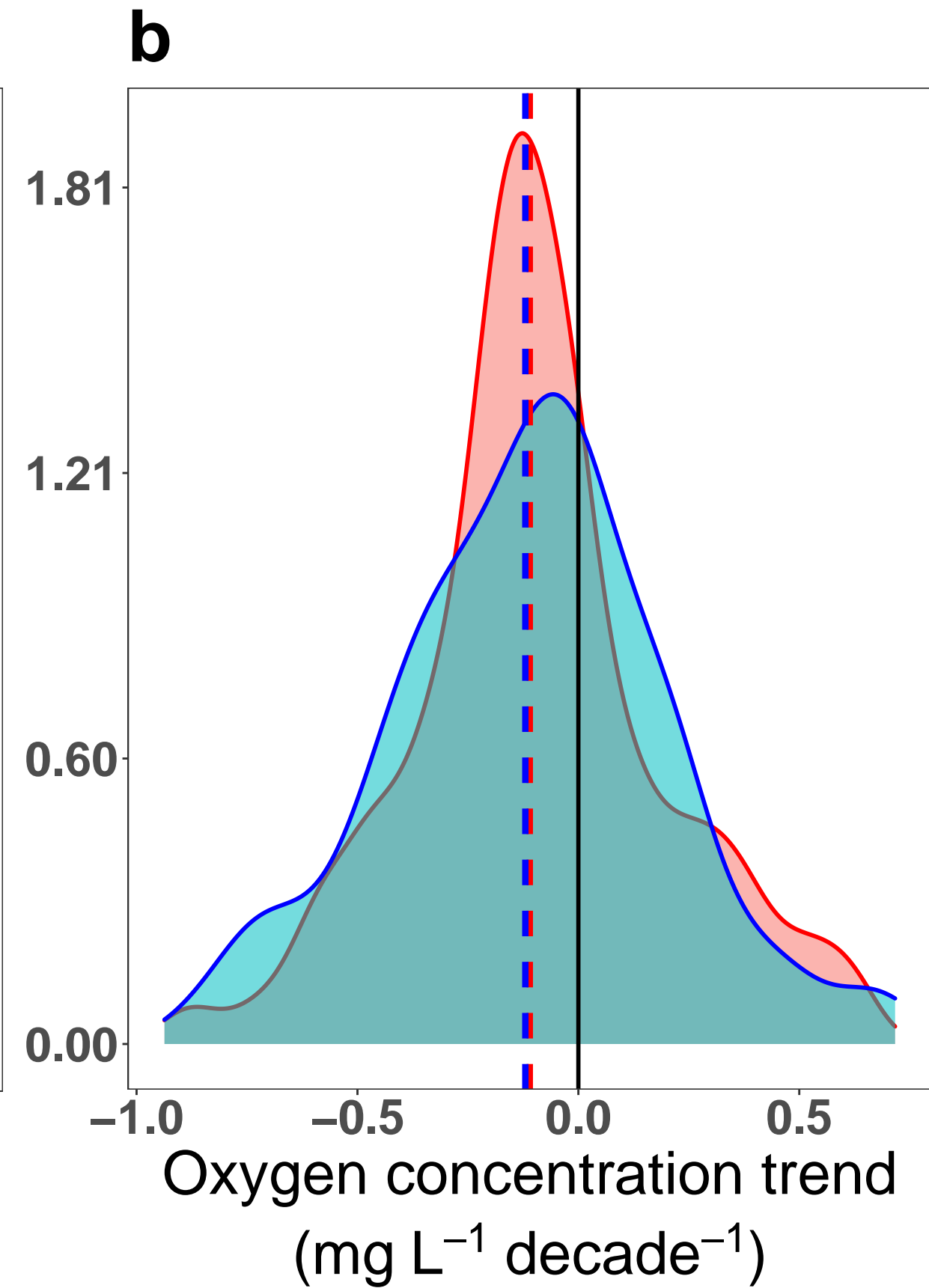
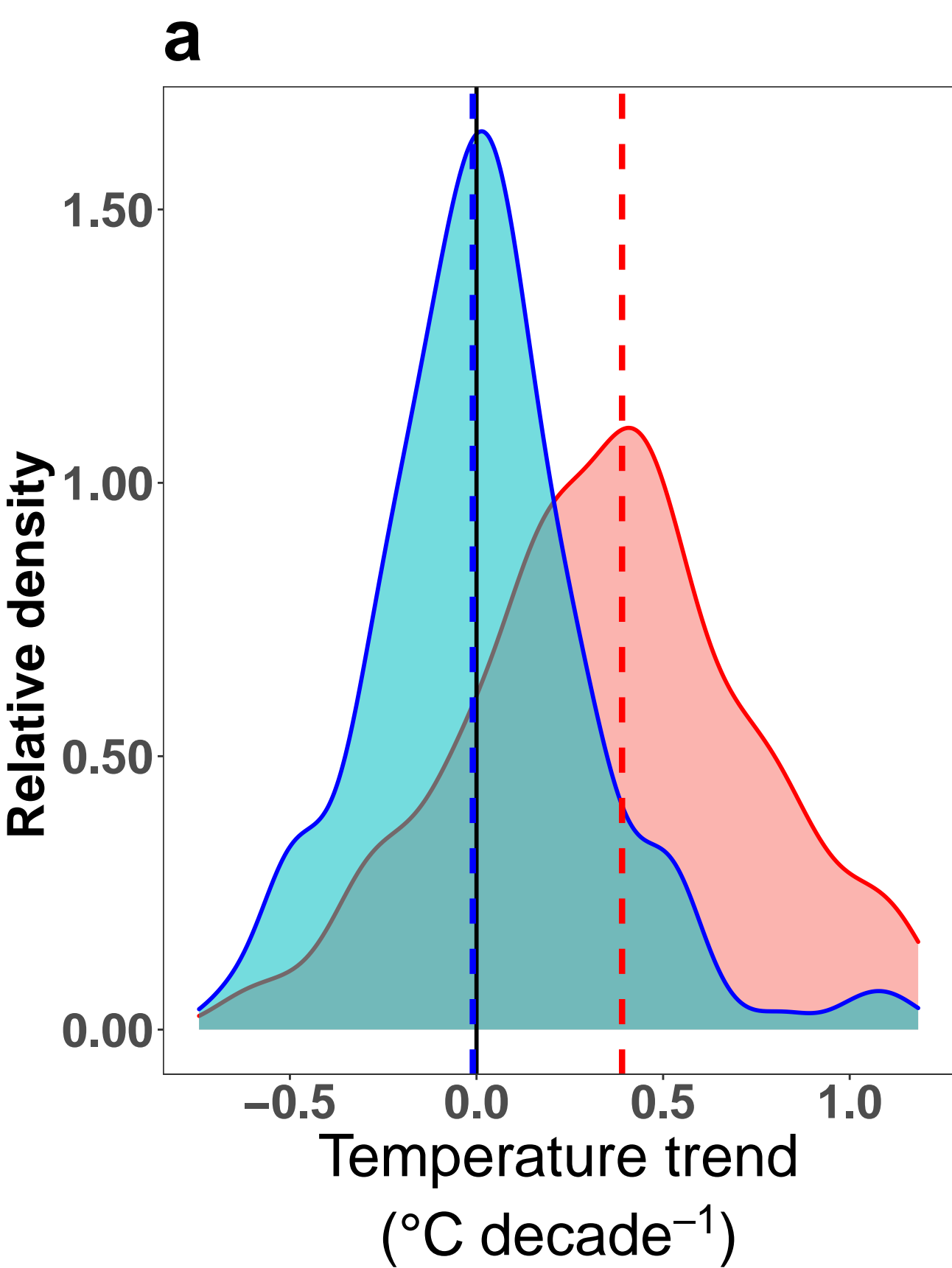
396 **Fig. 3 | Interaction of productivity and temperature in surface waters. a,** Predicted  
397 probability of a lake having both increasing surface temperature and DO concentration from a  
398 fitted logistic regression model at three different mean surface water temperatures:  $21^{\circ}\text{C}$  (blue),  
399  $25^{\circ}\text{C}$  (black),  $28^{\circ}\text{C}$  (red) **b,** Predictions of DO trends from a fitted multiple regression model for

400 chlorophyll (used as a surrogate for primary productivity) at these same temperatures (legend  
401 same as **a**) **c**, The interaction of water clarity (measured as Secchi depth in m) and surface-water  
402 temperature ( $^{\circ}\text{C}$ ) and their effects on surface DO ( $\text{mg L}^{-1}$ ) from fitted generalized additive mixed  
403 models (GAMM) **d**, Most lakes exhibited increasing surface temperatures and decreasing DO  
404 concentration consistent with solubility effects, but a subset of lakes ( $n = 87$ ) have both  
405 increasing surface temperature and DO concentration.

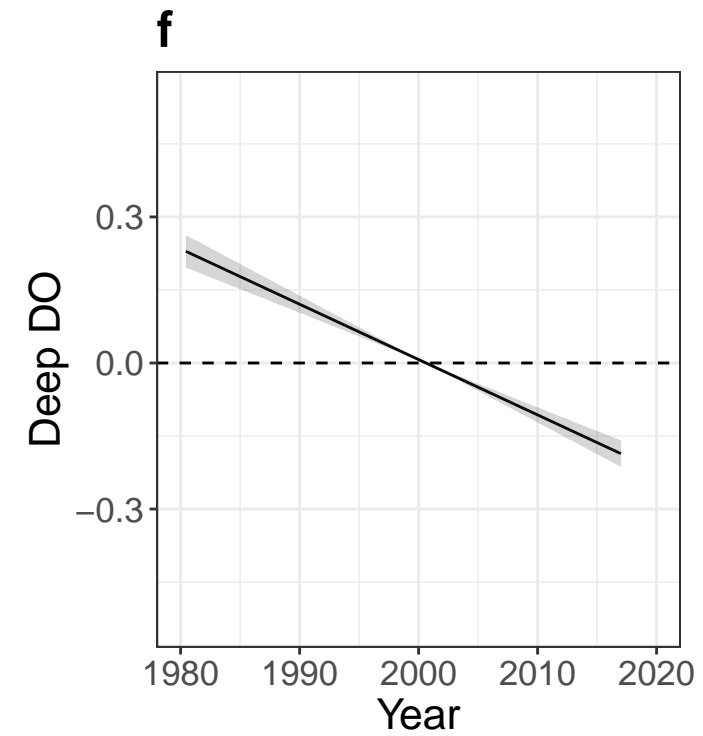
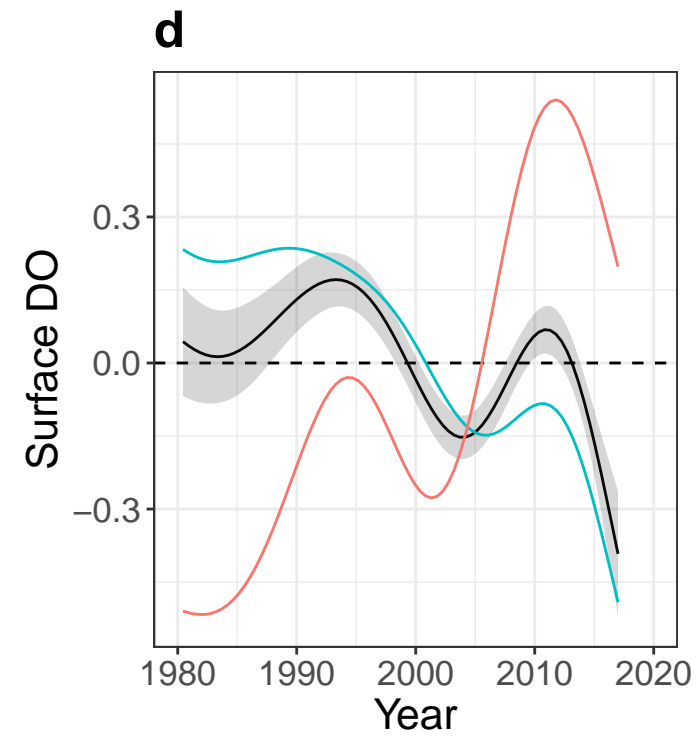
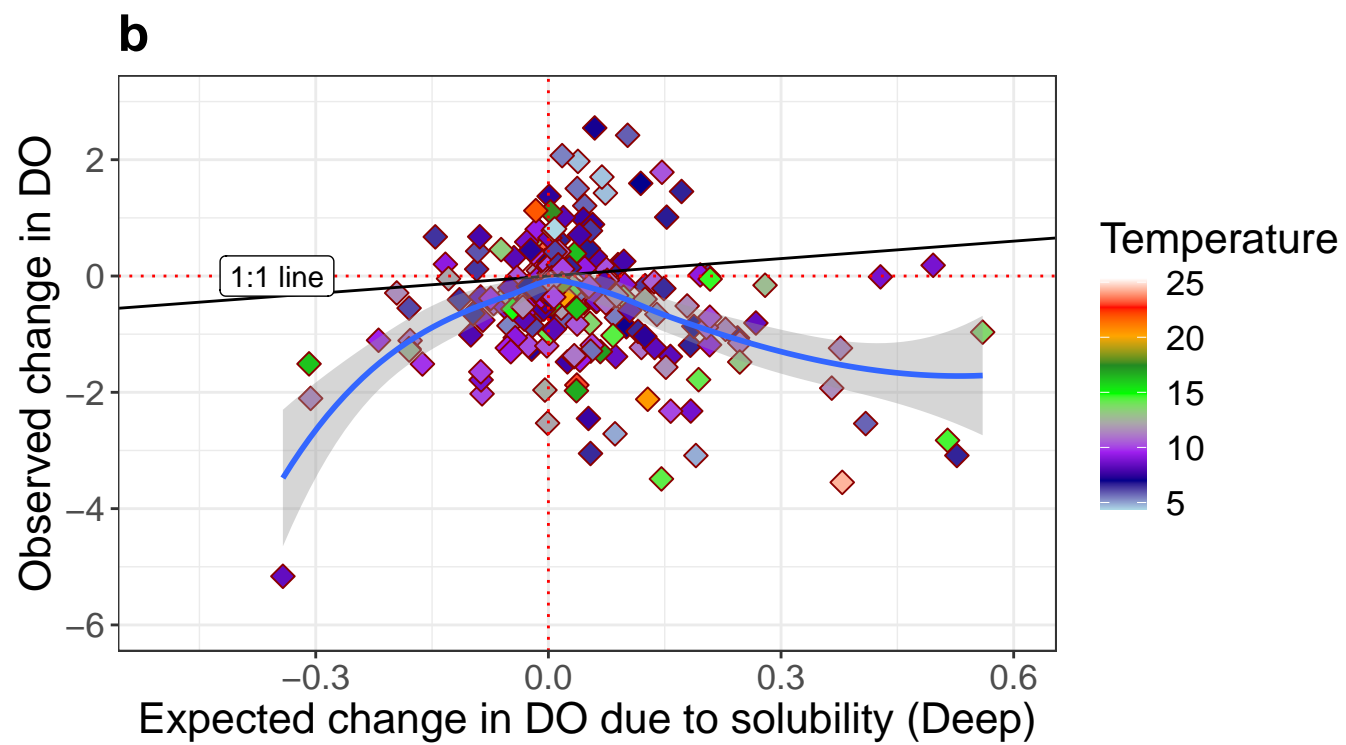
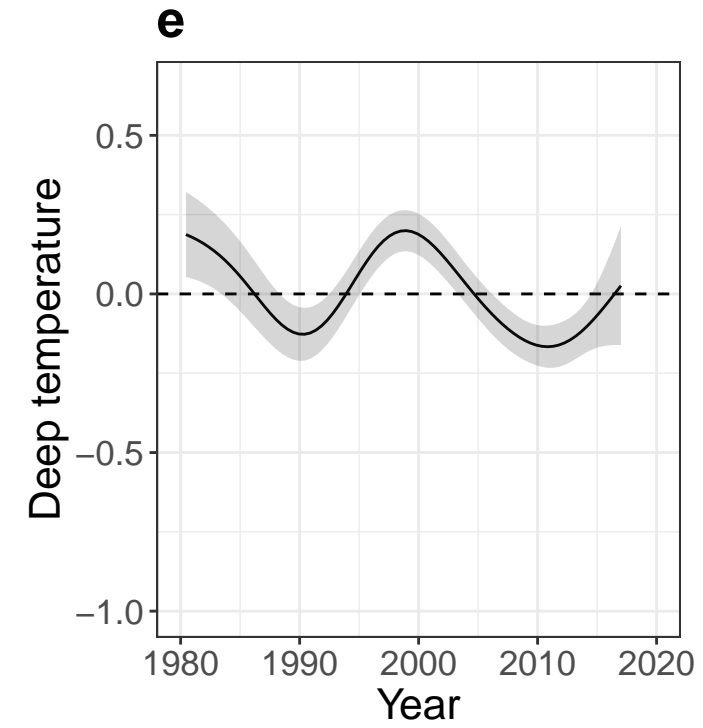
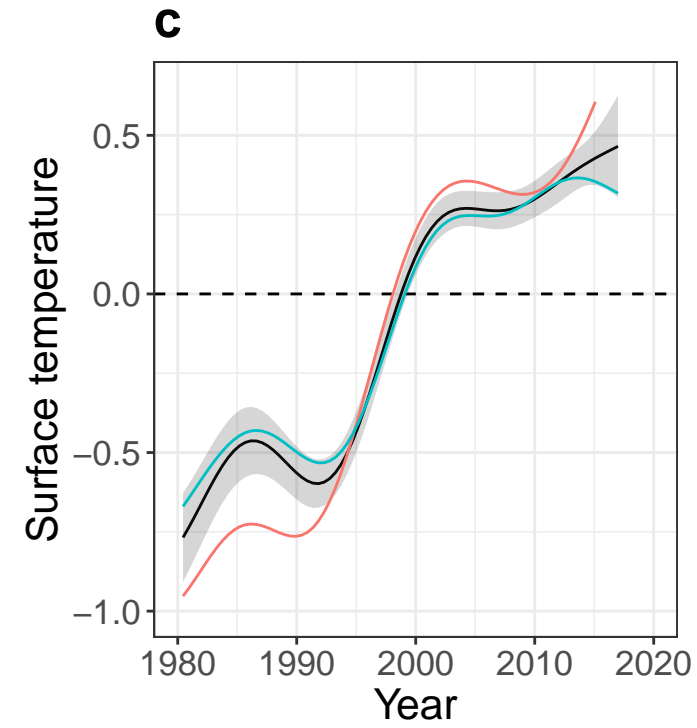
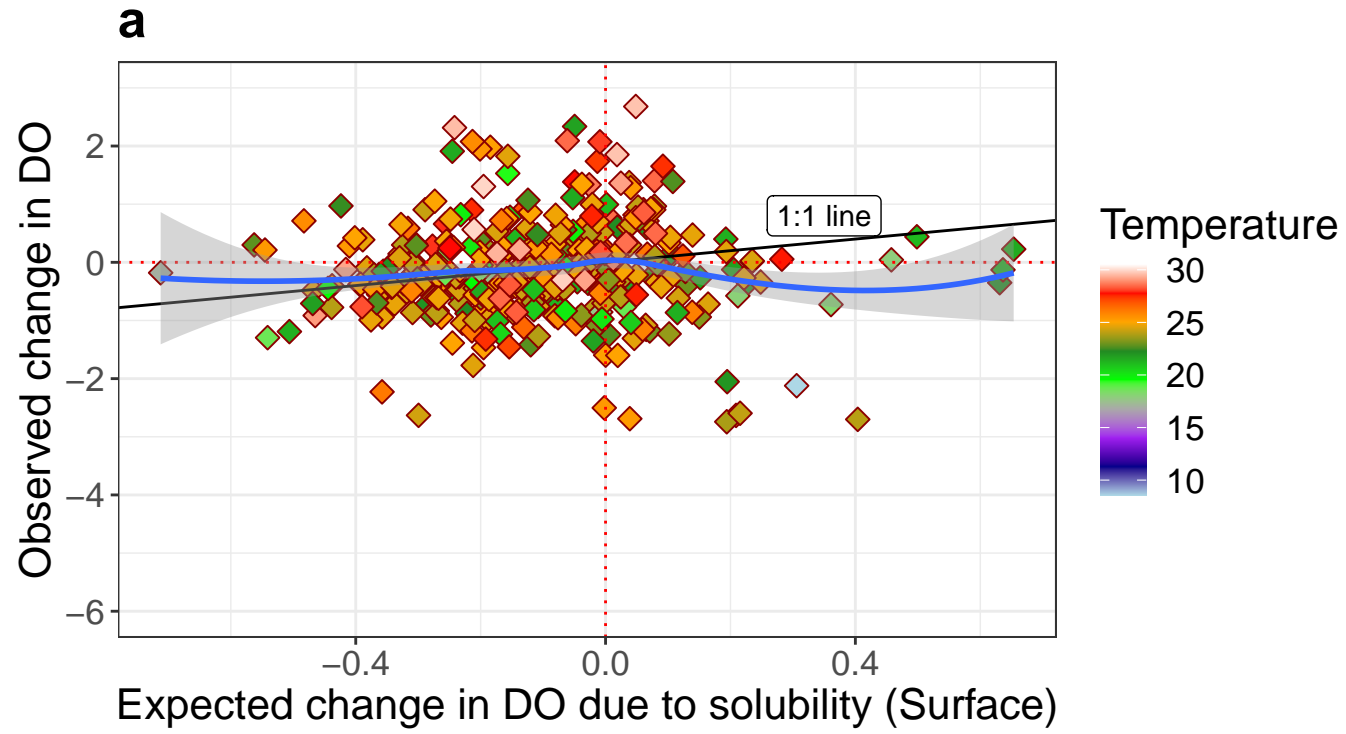
406

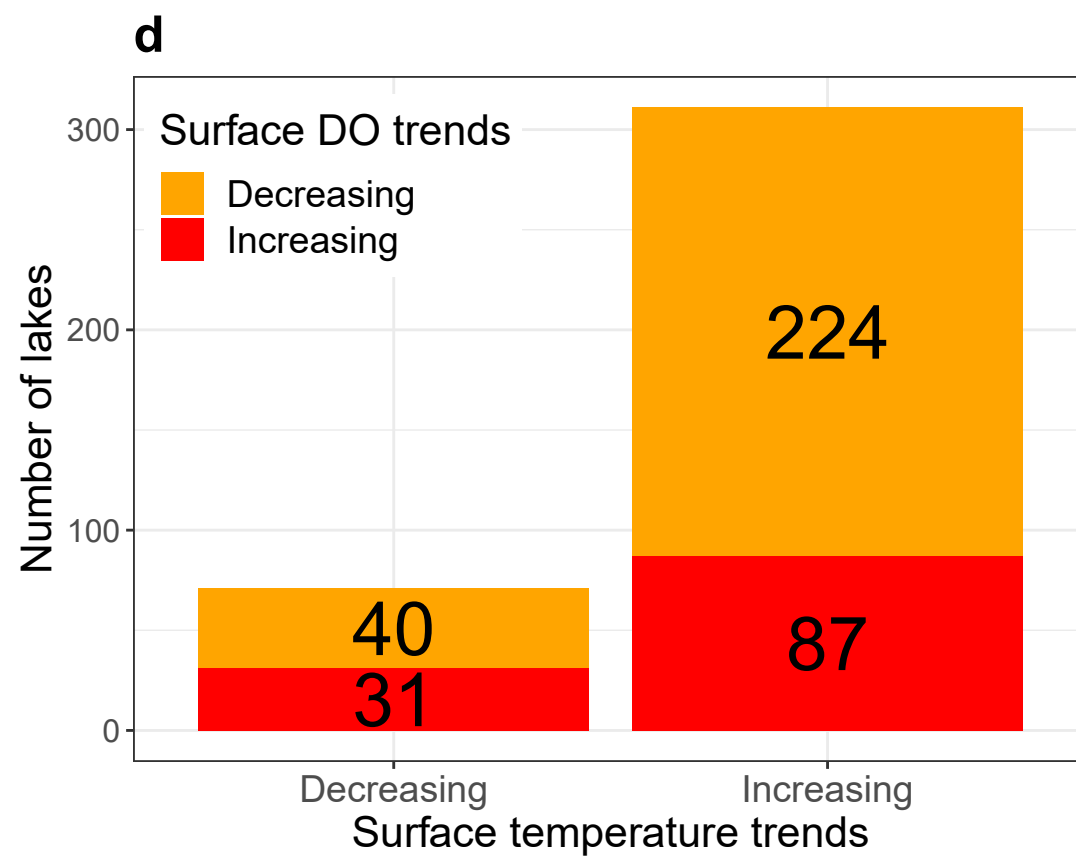
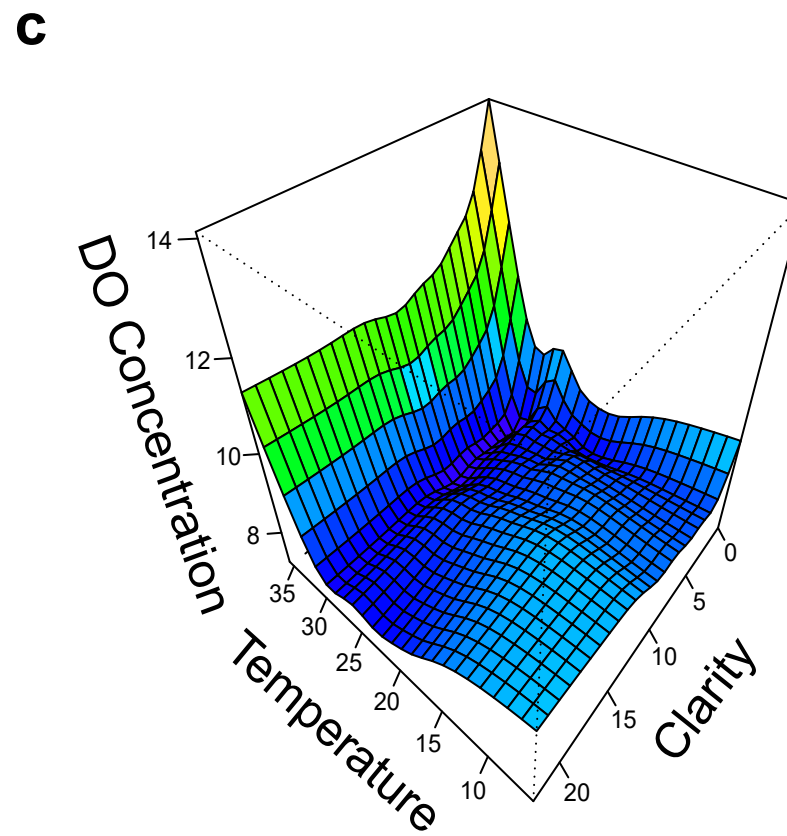
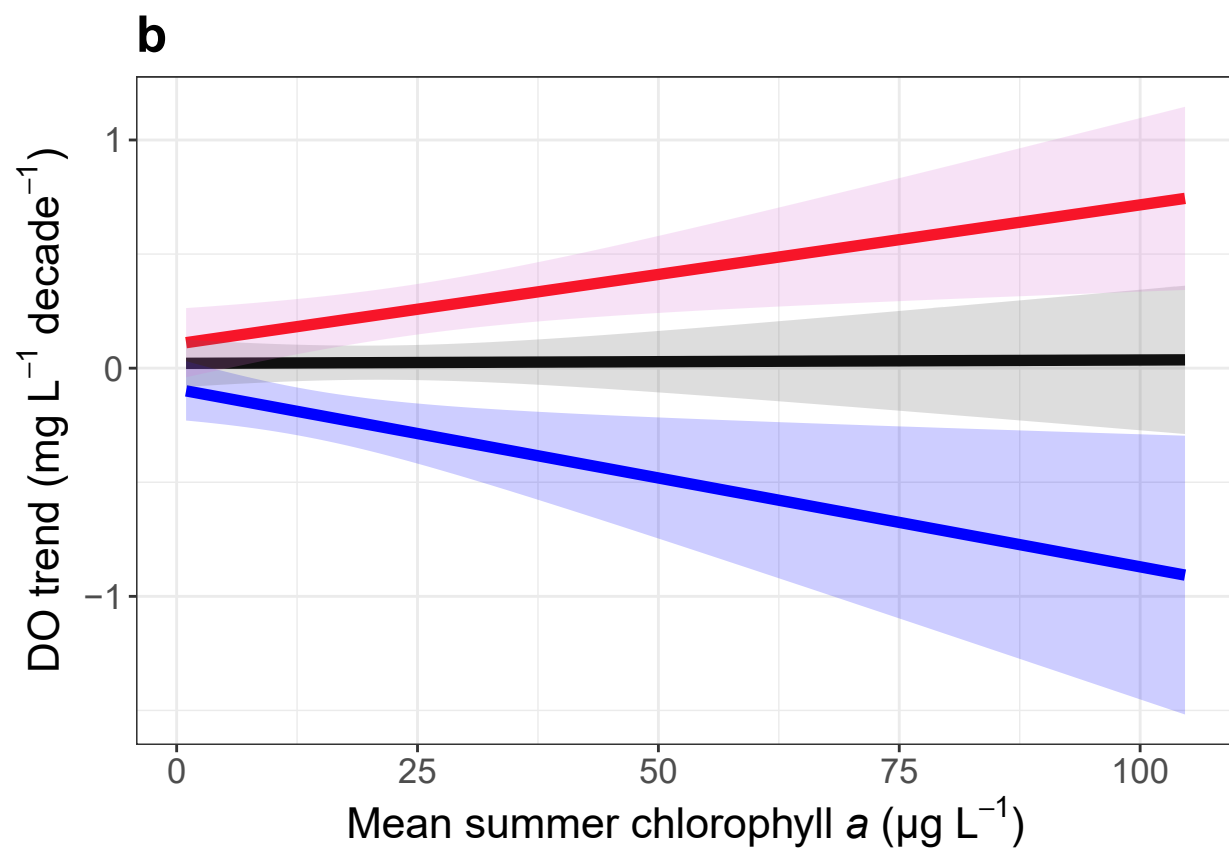
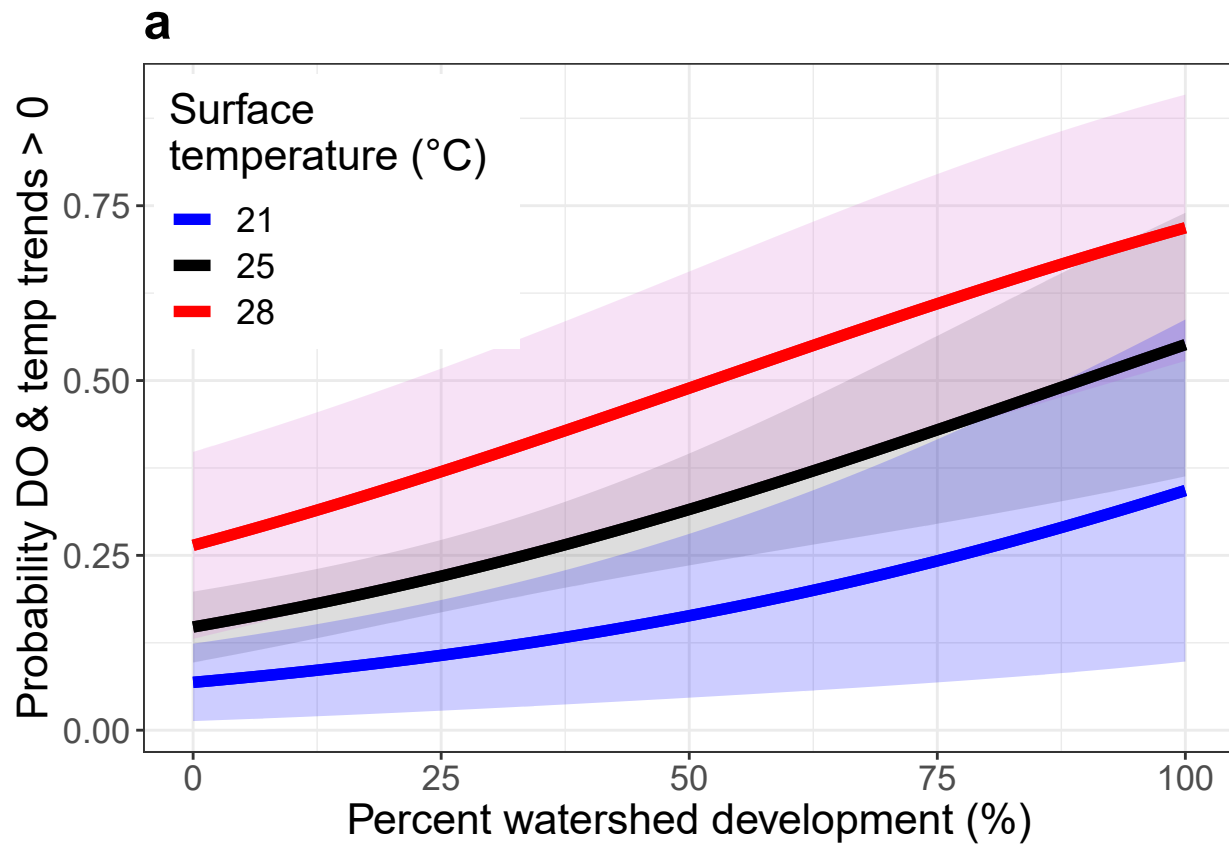
407 **Fig. 4 | Effect of changes in water clarity and density difference on deep-water DO**  
408 **saturation change. a**, Change in % saturation versus change in water clarity (Secchi depth). **b**,  
409 Change in % saturation versus change in water column density difference between surface and  
410 deep waters. The number of lakes in each quadrant in **a** and **b** are indicated by text. **c**, Predictions  
411 of change in % saturation from a fitted multiple regression model for change in water clarity at  
412 three density changes. **d**, Predictions of change in % saturation from a fitted multiple regression  
413 model for change in density difference at three clarity changes. Note that for both **c** and **d** the  
414 origin sits at no change in either predictor.

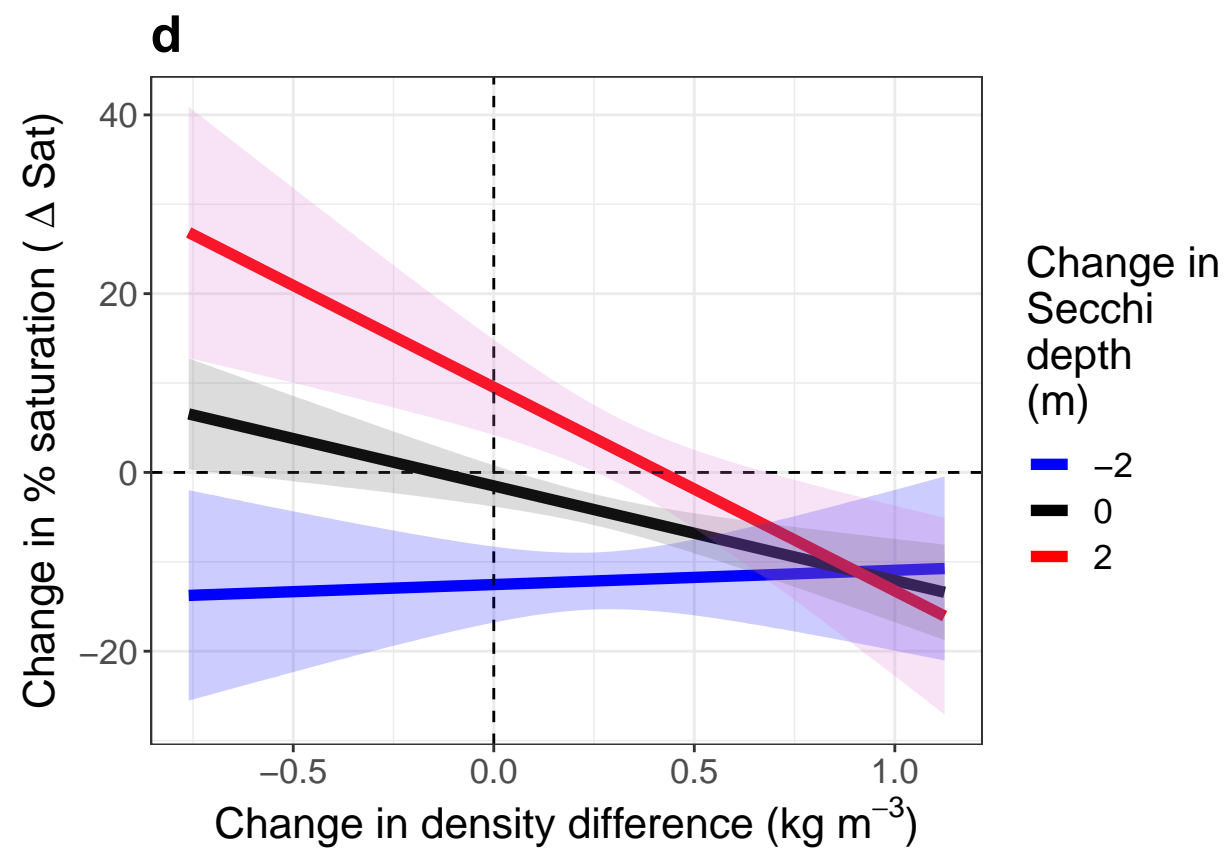
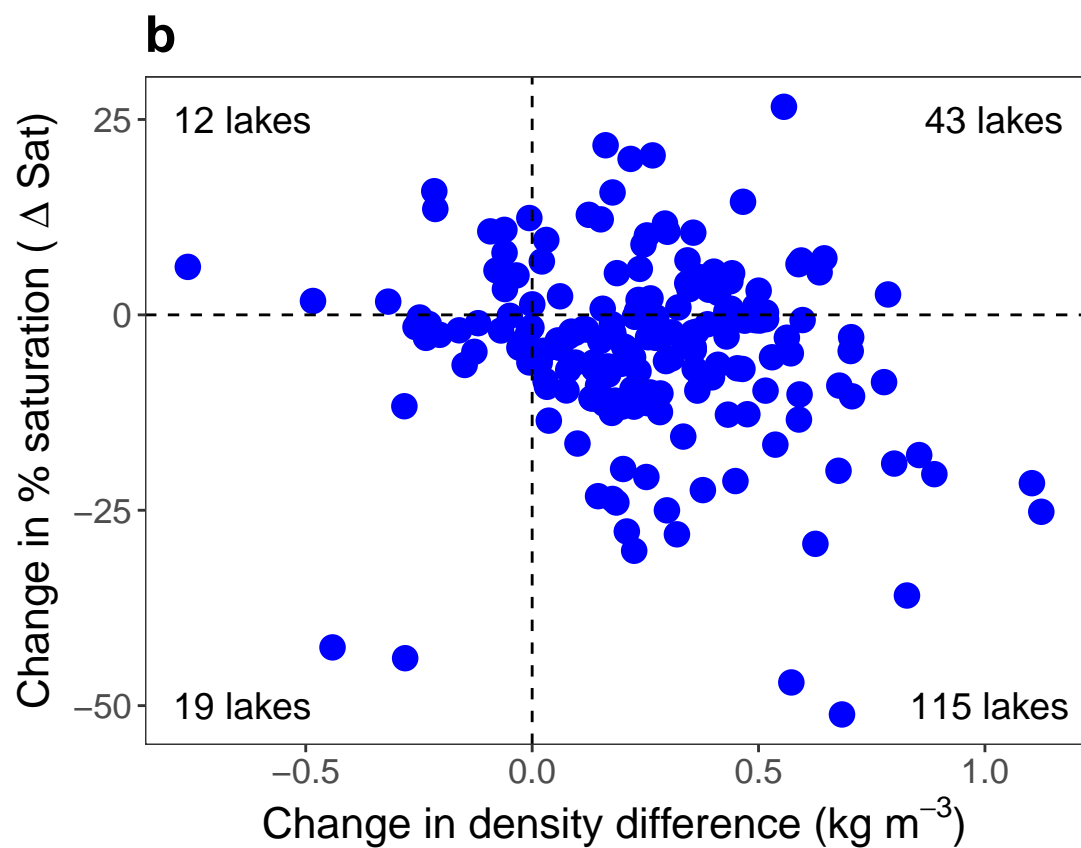
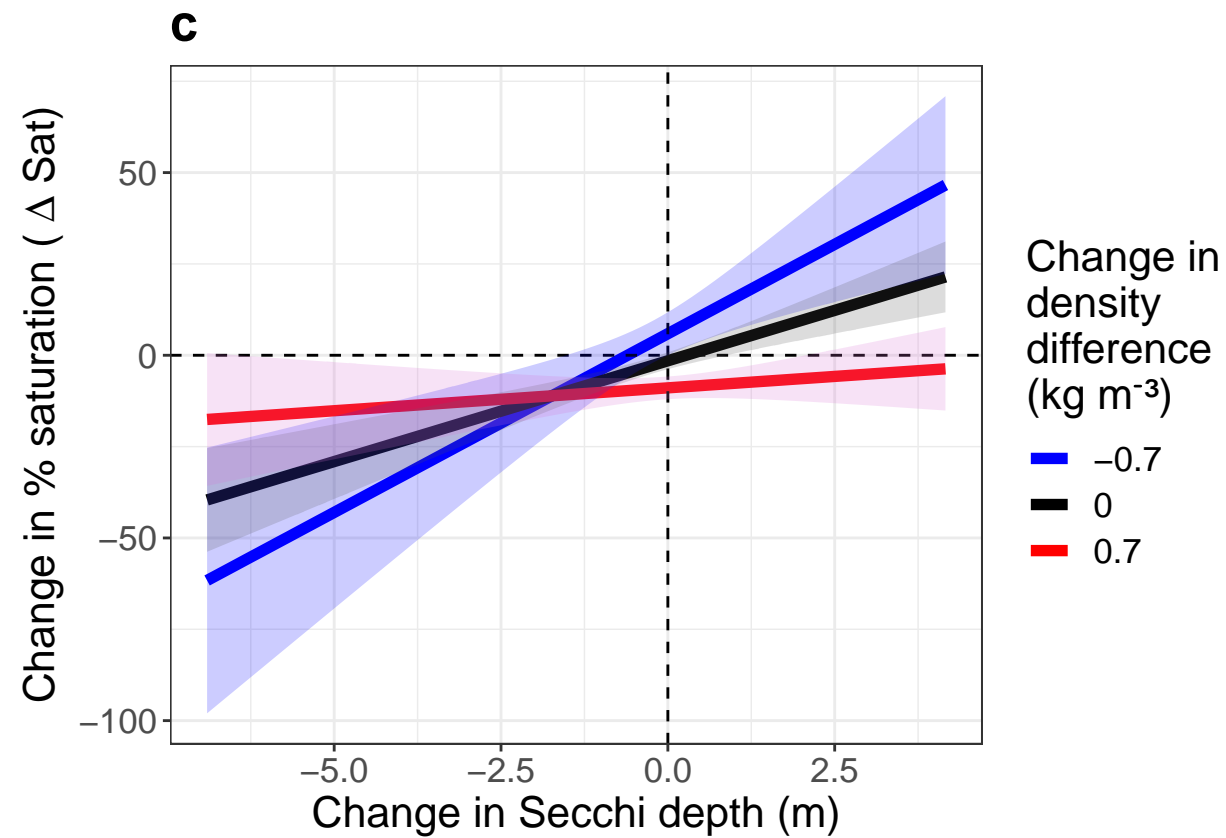
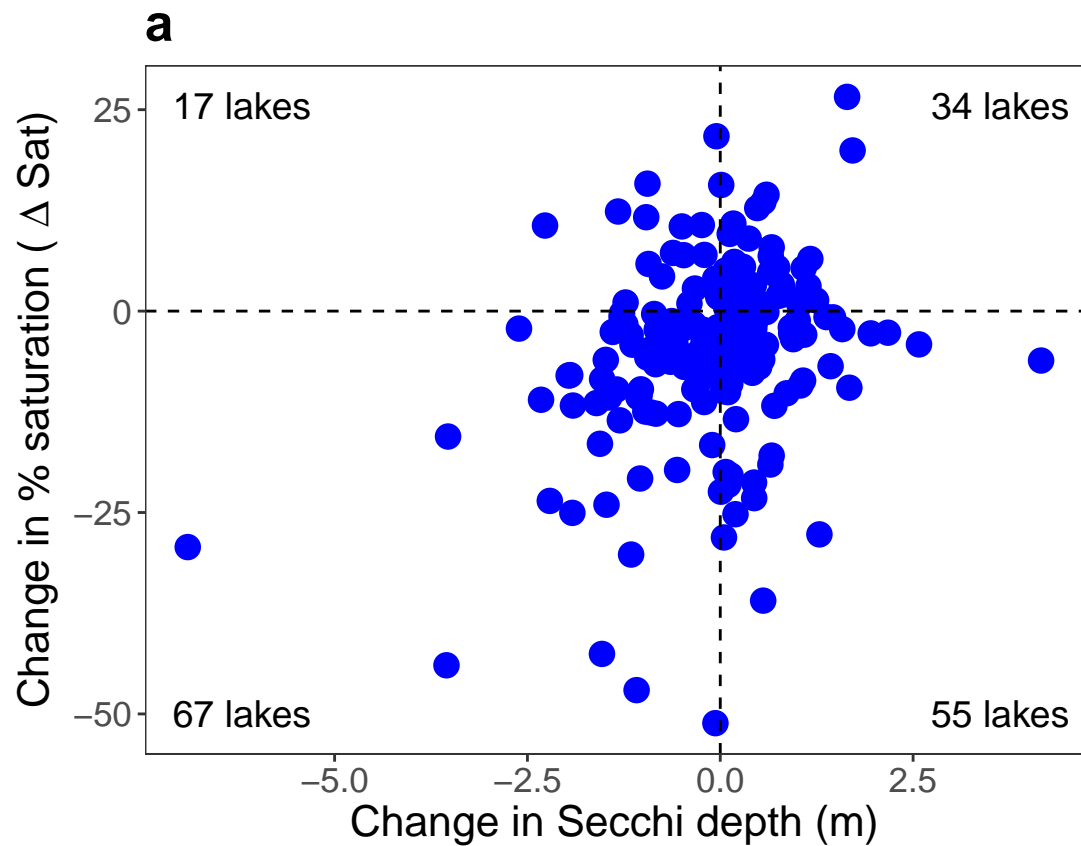
415











## 416 **Supplemental information**

417           There are seven supplemental information tables and four supplemental information  
418 figures. Tables S1 and S2 are referenced in text. Table S3 describes data contributors for this  
419 project and Table S4 provides location and trend information for each lake. Trend data were not  
420 reported for a) two lakes where providers did not provide permission to publish data but that  
421 were included in trend analyses (Annecy and Geneva; ‘NP’ in table S4), b) lakes had less than 15  
422 years of data at a given depth (not shown in table), or c) deep-water trends in lakes that did not  
423 thermally stratify (‘NA’ in table S4). In one lake (T Bird), epilimnetic water was artificially  
424 aerated and this depth layer was excluded from analysis. Table S5 presents statistics associated  
425 with spatial autocorrelation analyses. Table S6 describes trends over the entire population of  
426 lakes versus a sub-sample of lakes after accounting for the large numbers of samples obtained in  
427 lake-rich regions. Table S7 describes trends and uncertainty in trends over two time periods for  
428 subsets of lakes having data for at least 80% of years: 1980-2017 and 1990-2017. Fig. S1  
429 presents the results of GAMM analysis of trends zoomed out to visualize distribution of residuals  
430 for surface and deep-water temperature and dissolved oxygen trends. Fig. S2 presents the partial  
431 dependency plots for the top predictors of changes in deep-water DO percent saturation as  
432 determined by a random forest analysis. Fig. S3 presents partial dependency plots for the top  
433 predictors of changes in water column density difference between surface and deep waters as  
434 determined by a random forest analysis. Fig. S4 presents the locations of lakes used in this study  
435 (n=393).

436

437 **Figure S1** | Results of GAMM analysis of trends zoomed out to visualize distribution of  
438 residuals. **a**, Surface-water temperature (°C) **b**, Deep-water temperature (°C) **c**, Surface-water  
439 DO (mg L<sup>-1</sup>) and **d**, Deep-water DO concentration (mg L<sup>-1</sup>).

440

441 **Figure S2** | **a-f**, Partial dependency plots from a random forest algorithm of deep-water change  
442 in % dissolved oxygen saturation ( $\Delta$  Sat) in the last five years of record relative to the first five  
443 years of record for each lake. Plots are ordered by predictor variable importance, decreasing in  
444 importance from the upper left to lower right (a to f). Vertical red lines indicate zero change in  
445 predictor variable and hash marks on the x-axis indicate lake distribution deciles. Partial  
446 dependencies indicate the relationship between predictor and response variables when holding  
447 other variables at their mean value. Lakes that experienced no change in either water clarity or  
448 density difference between surface and deep waters exhibited little change in deep-water  
449 saturation (see also, Fig. 4).

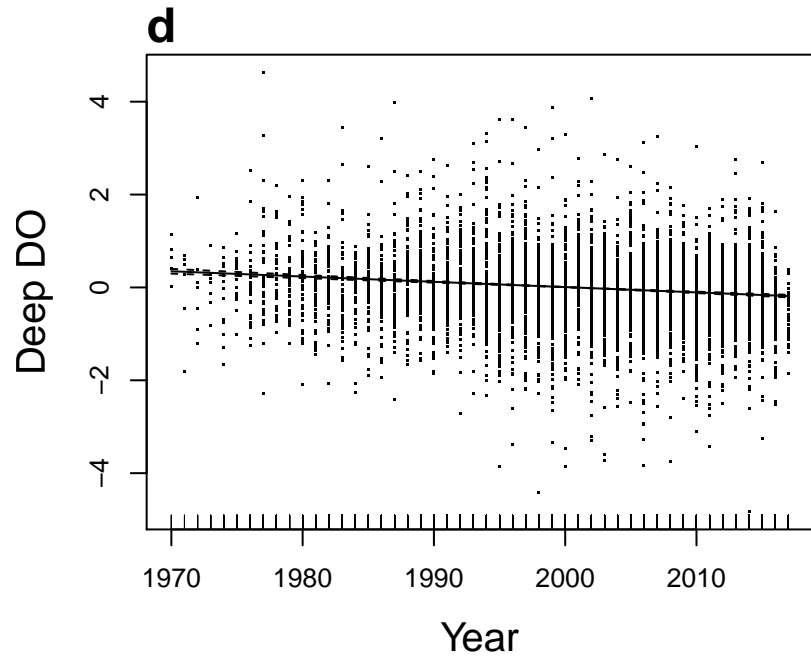
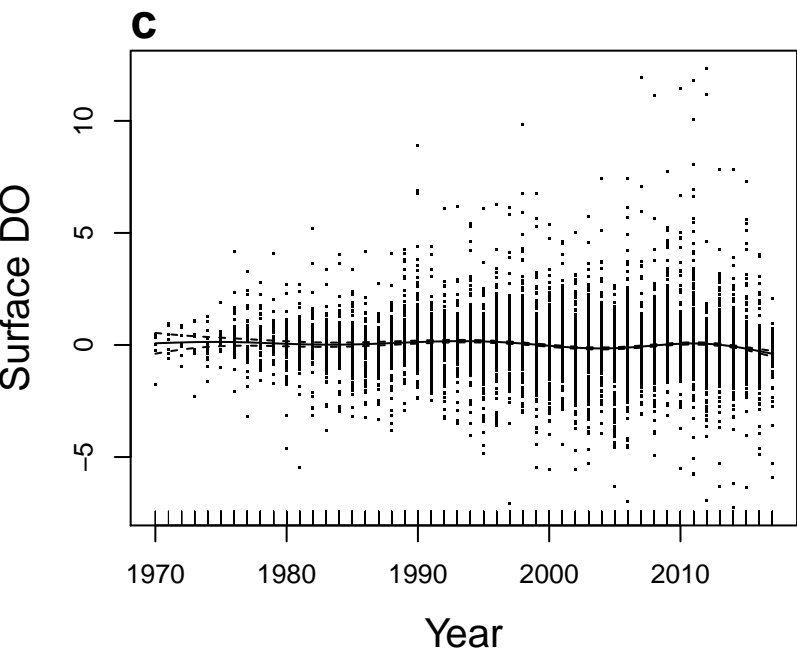
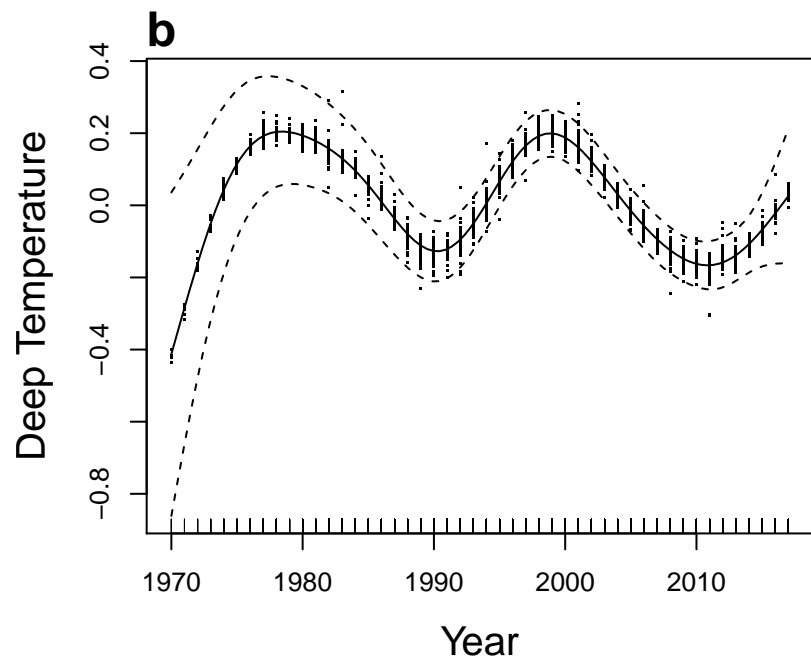
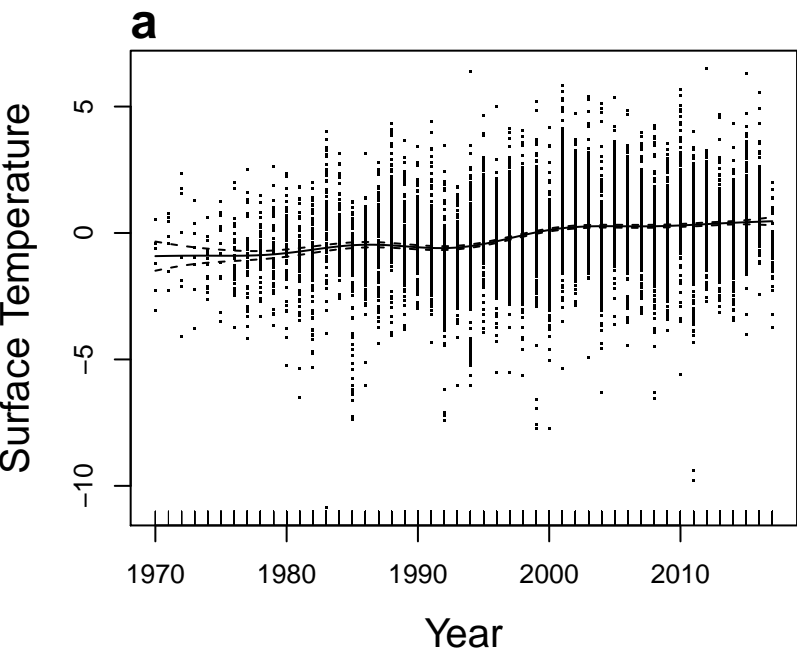
450

451 **Figure S3** | Drivers of the change in density difference between surface and deep waters. **a-f**,  
452 Partial dependency plots from a random forest algorithm of deep-water change in water column  
453 density difference in the last five years of record relative to the first five years of record for each  
454 lake. Plots are ordered by predictor variable importance, decreasing in importance from the  
455 upper left to lower right (a to f). Vertical red lines indicate zero values for predictor variable and  
456 hash marks on the x-axis indicate lake distribution deciles. Partial dependencies indicate the  
457 relationship between predictor and response variables when holding other variables at their mean  
458 value.

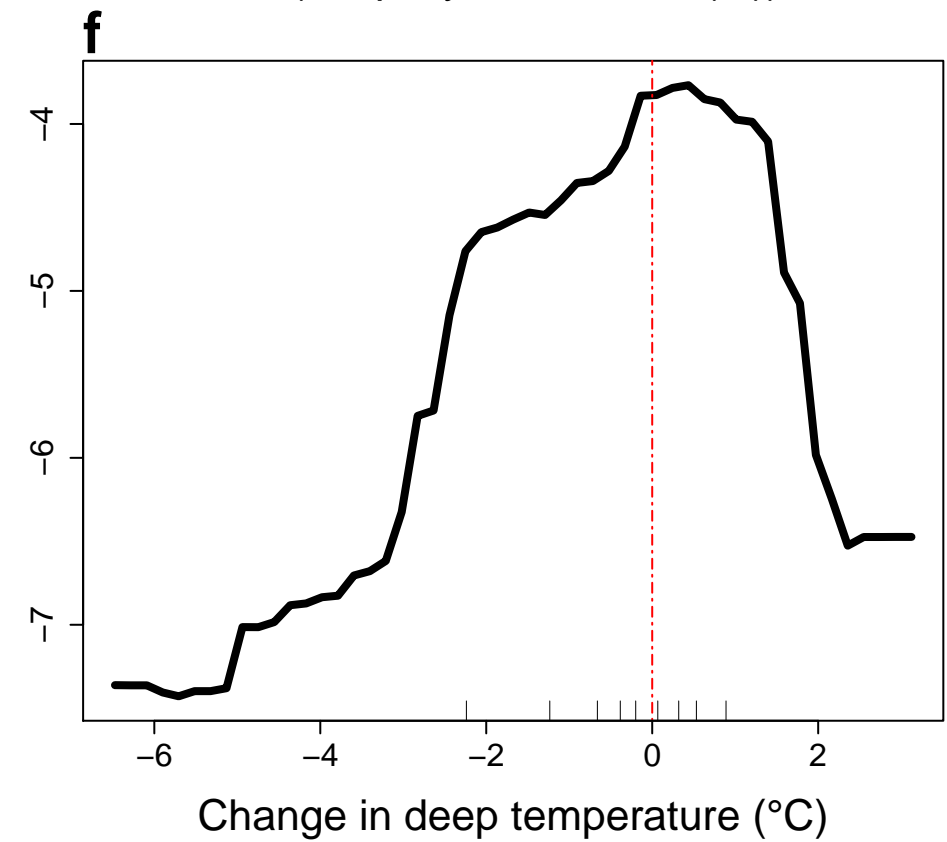
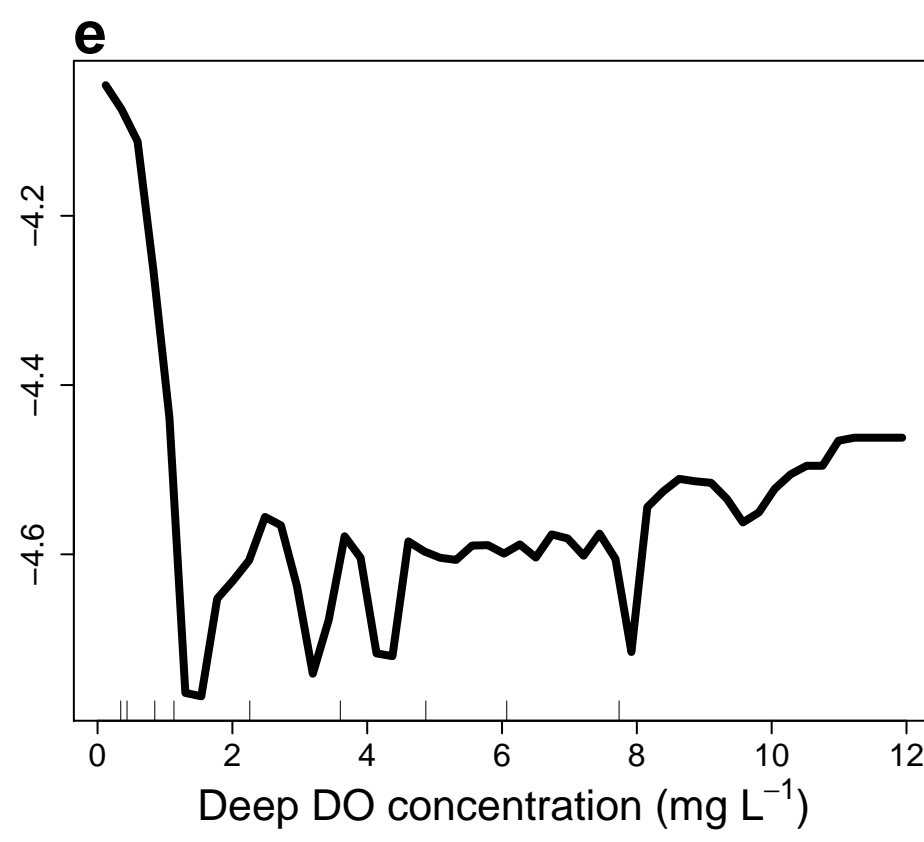
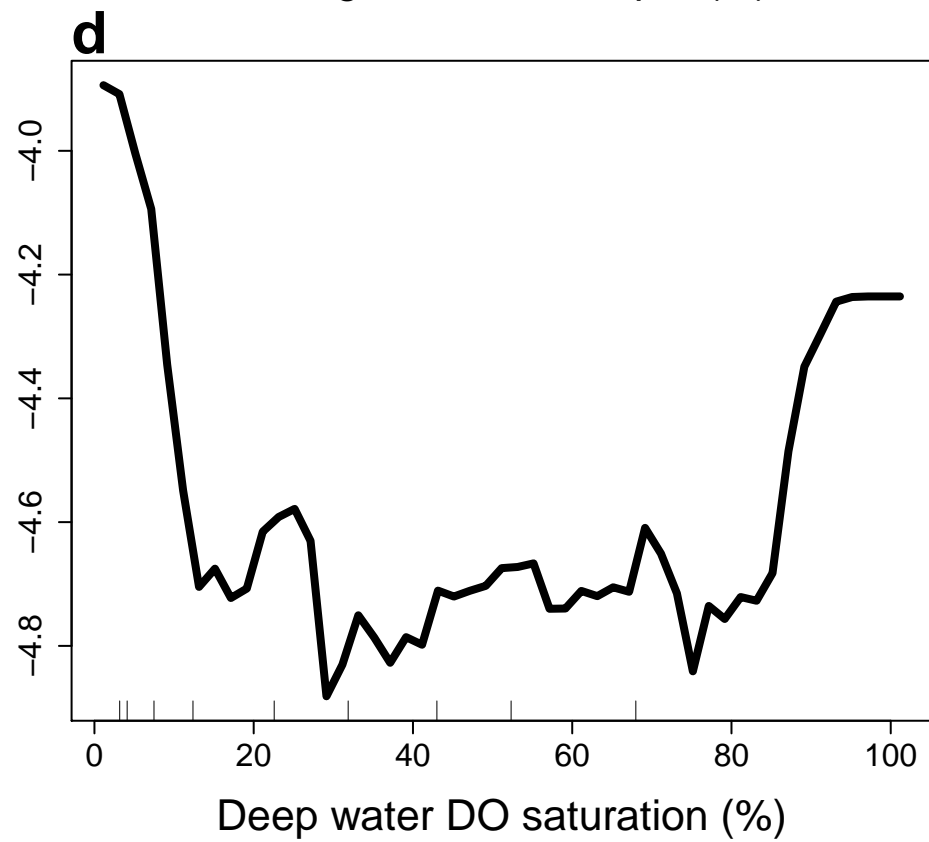
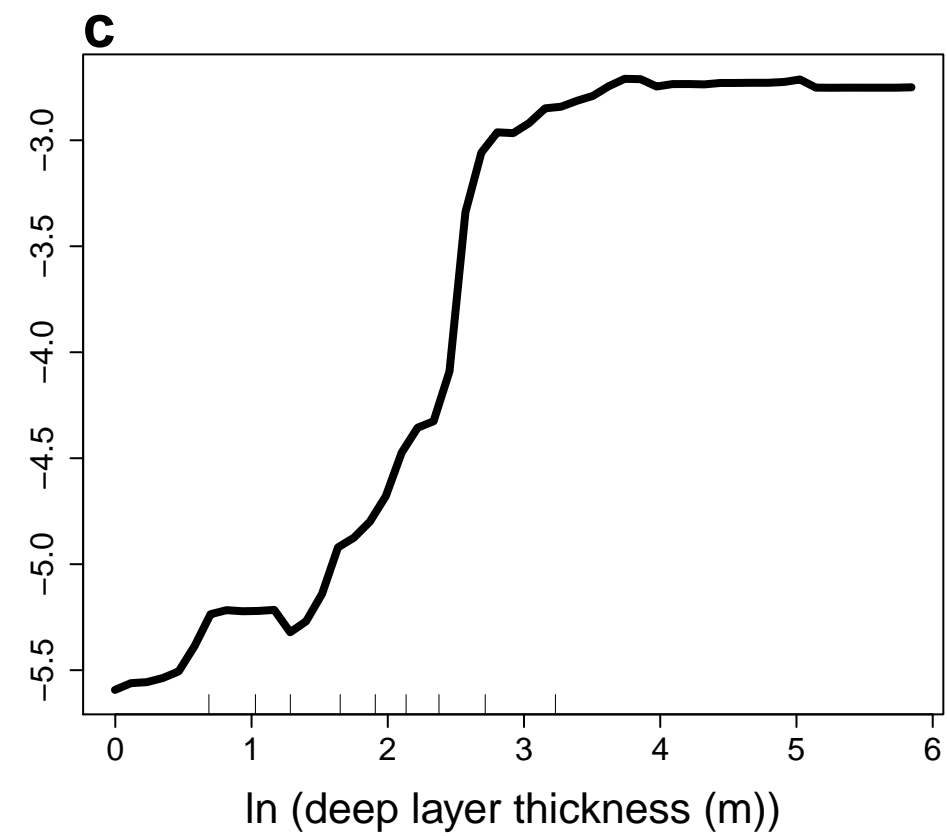
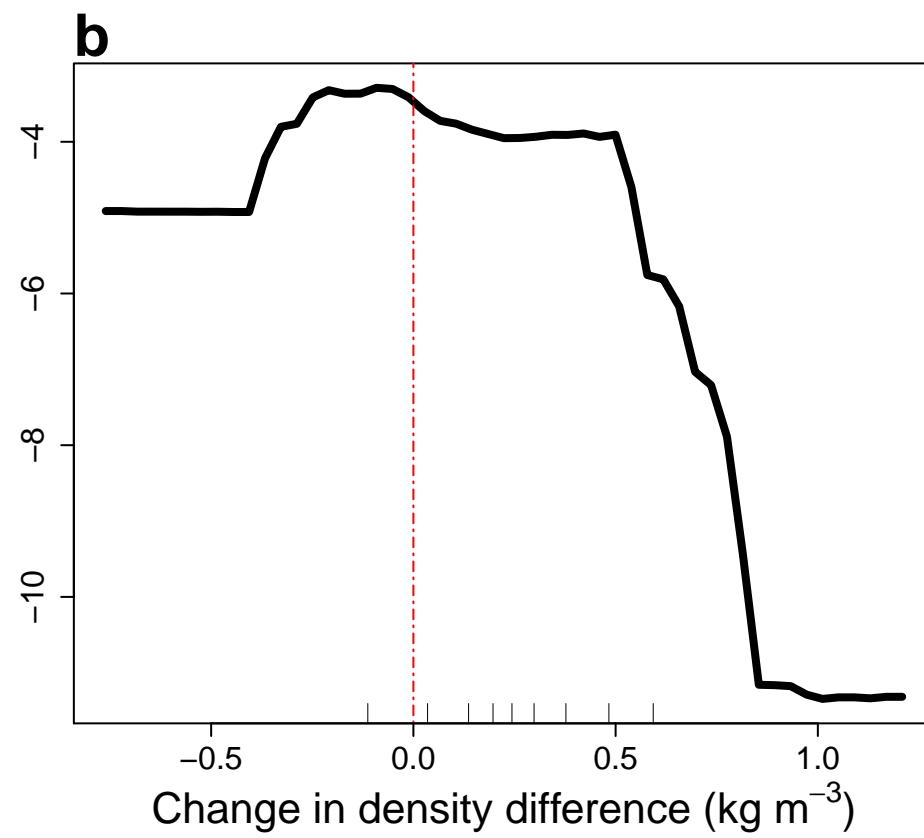
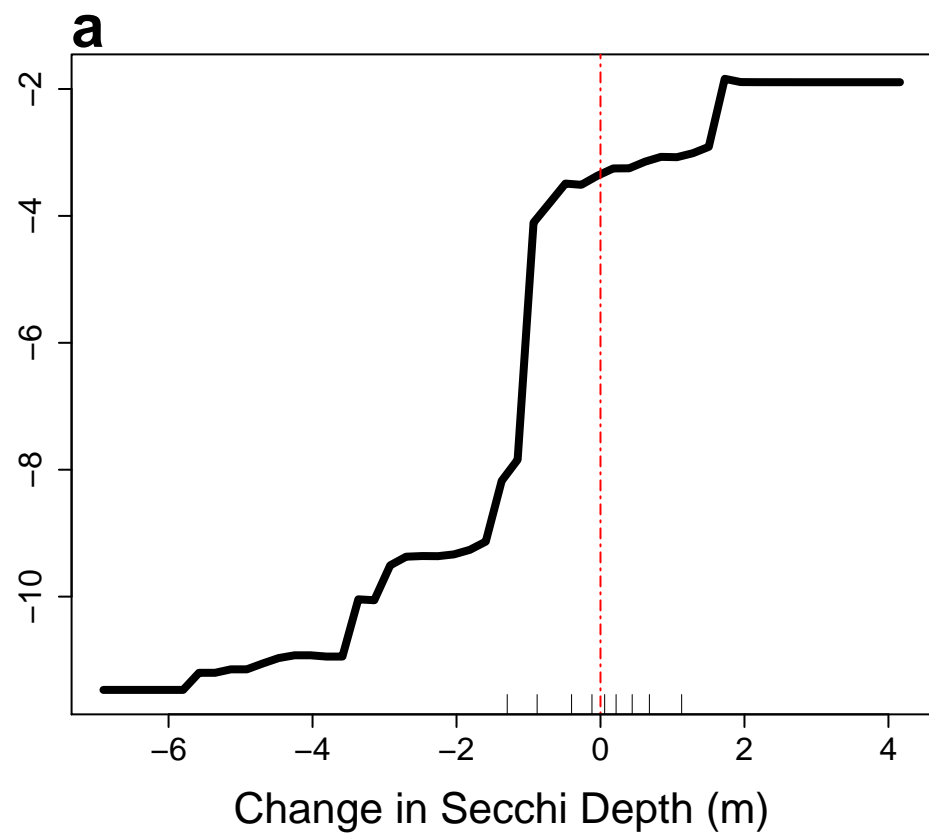
459

460 **Fig. S4** | Locations of lakes used in this study (n=393).

461

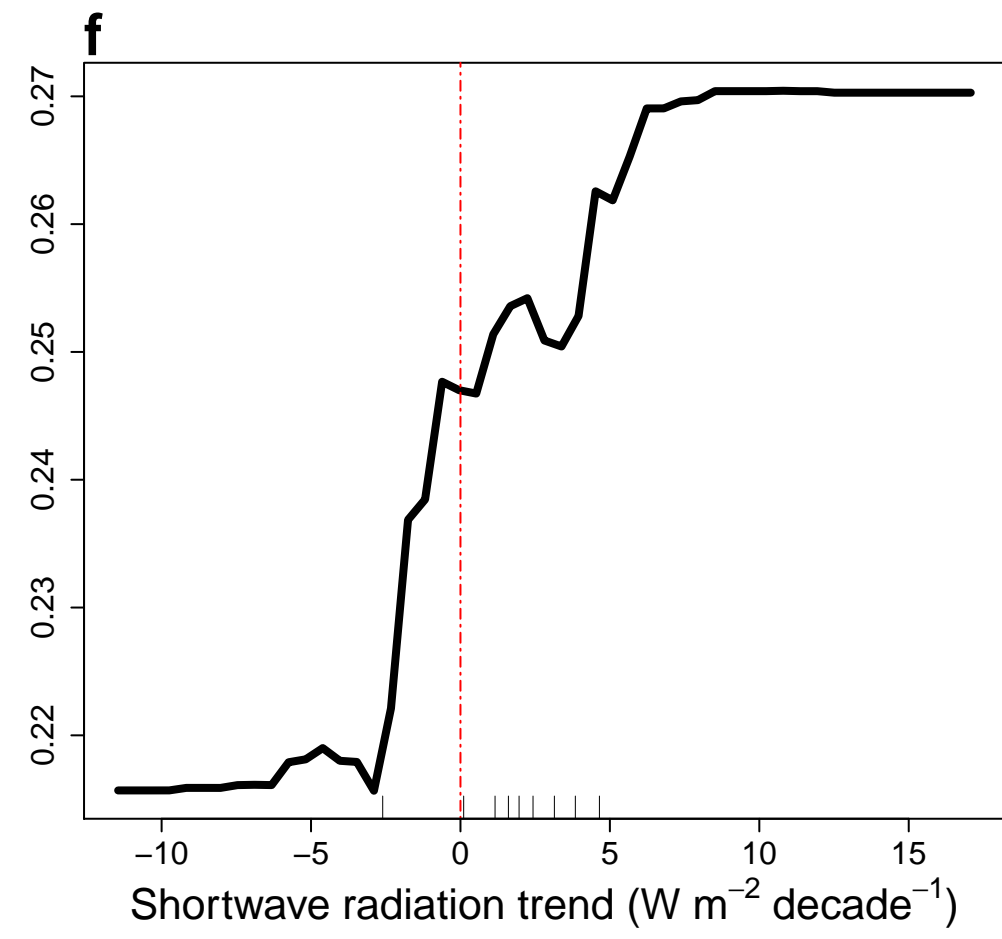
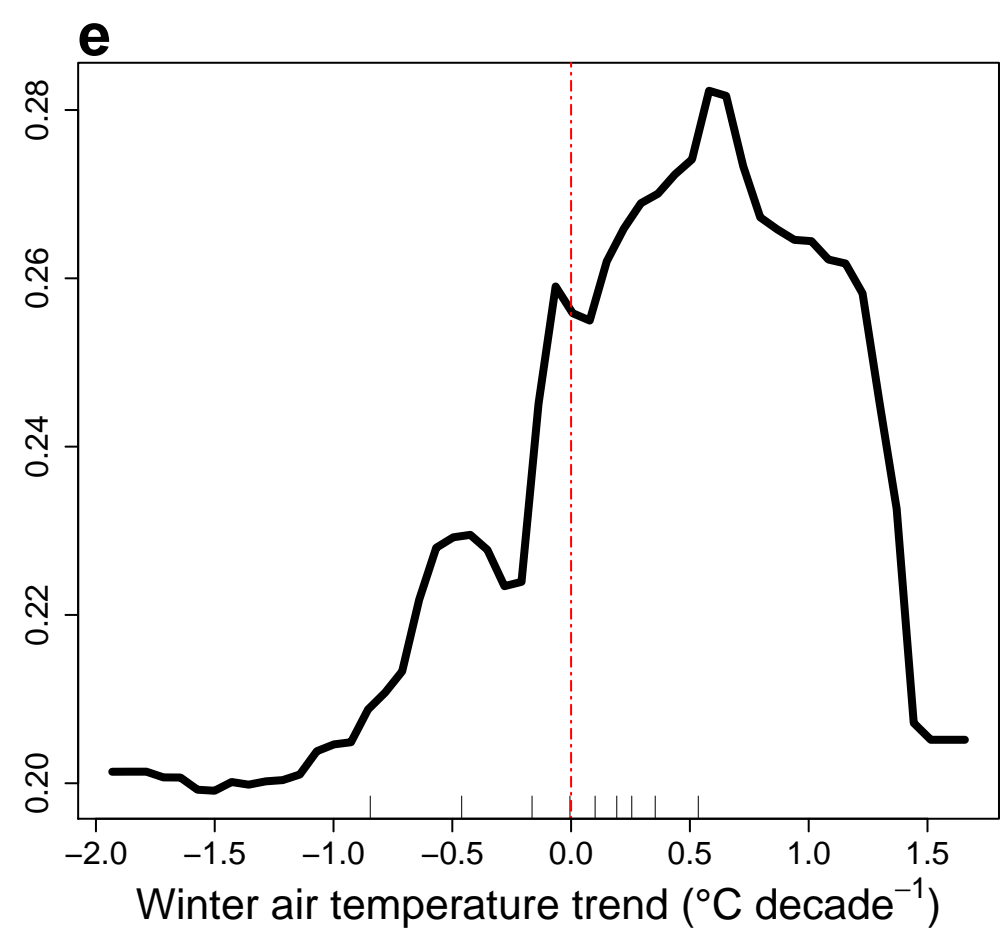
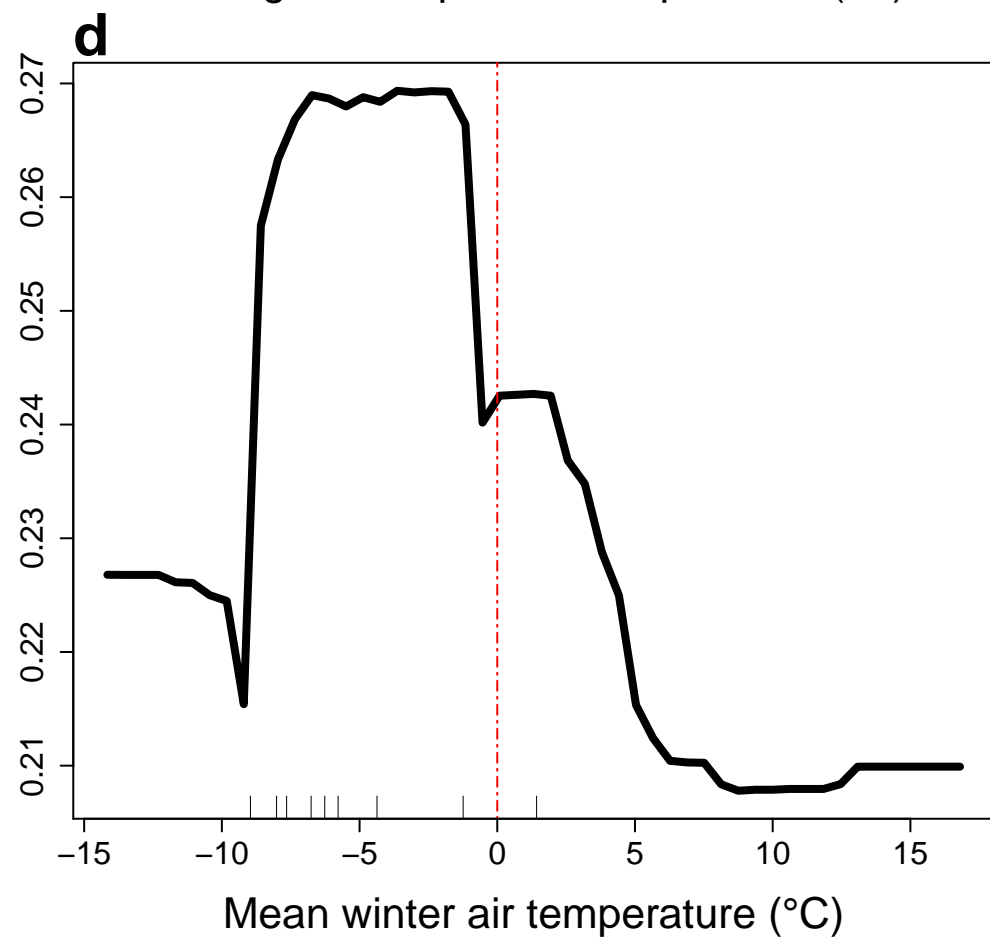
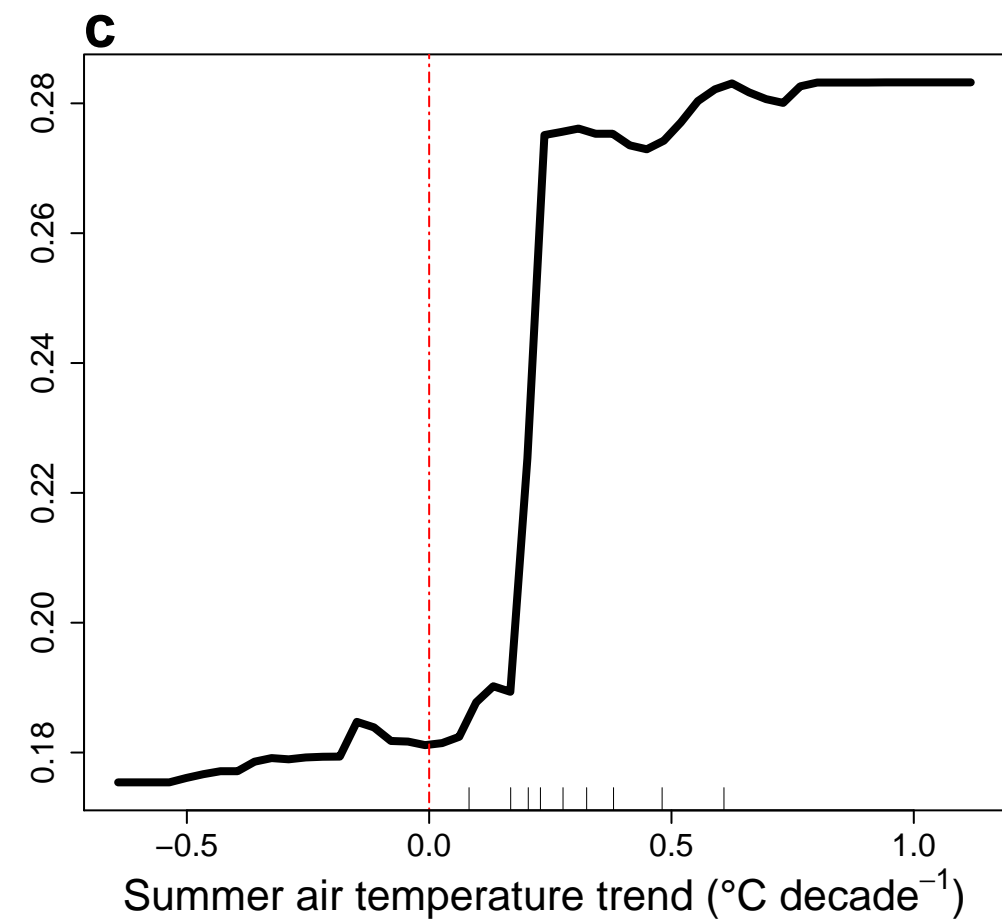
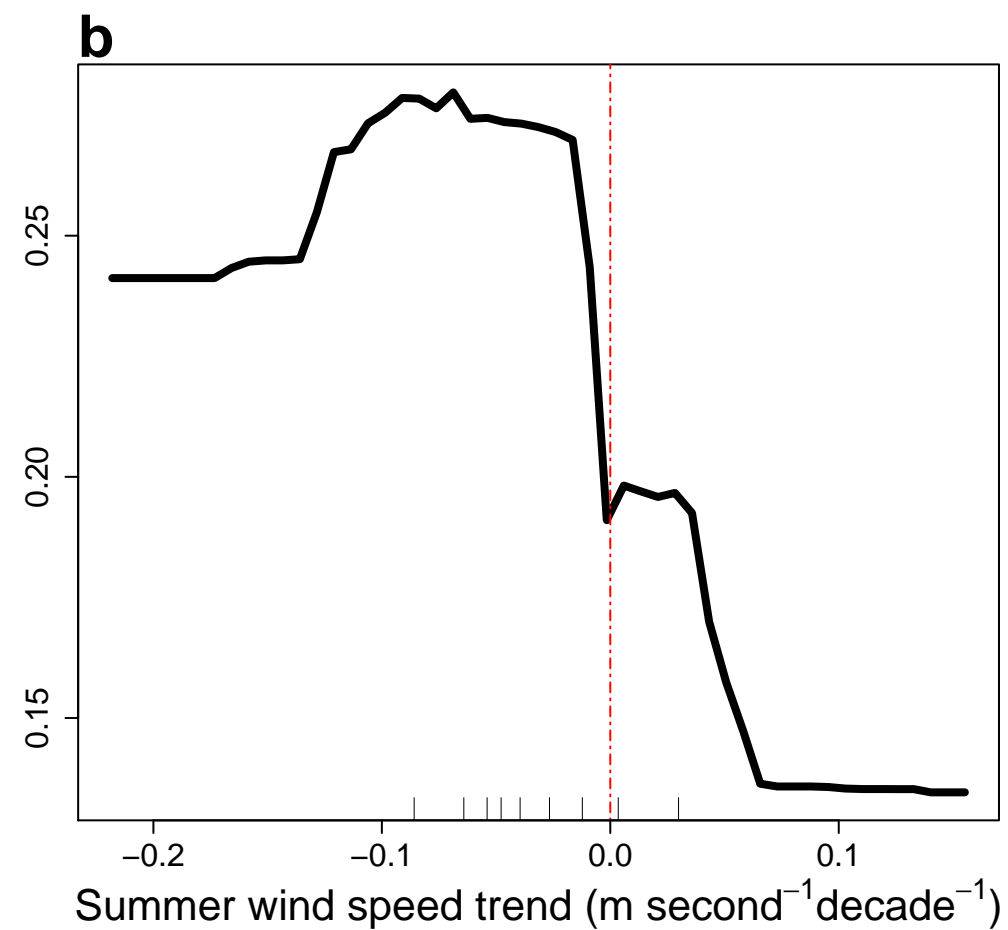
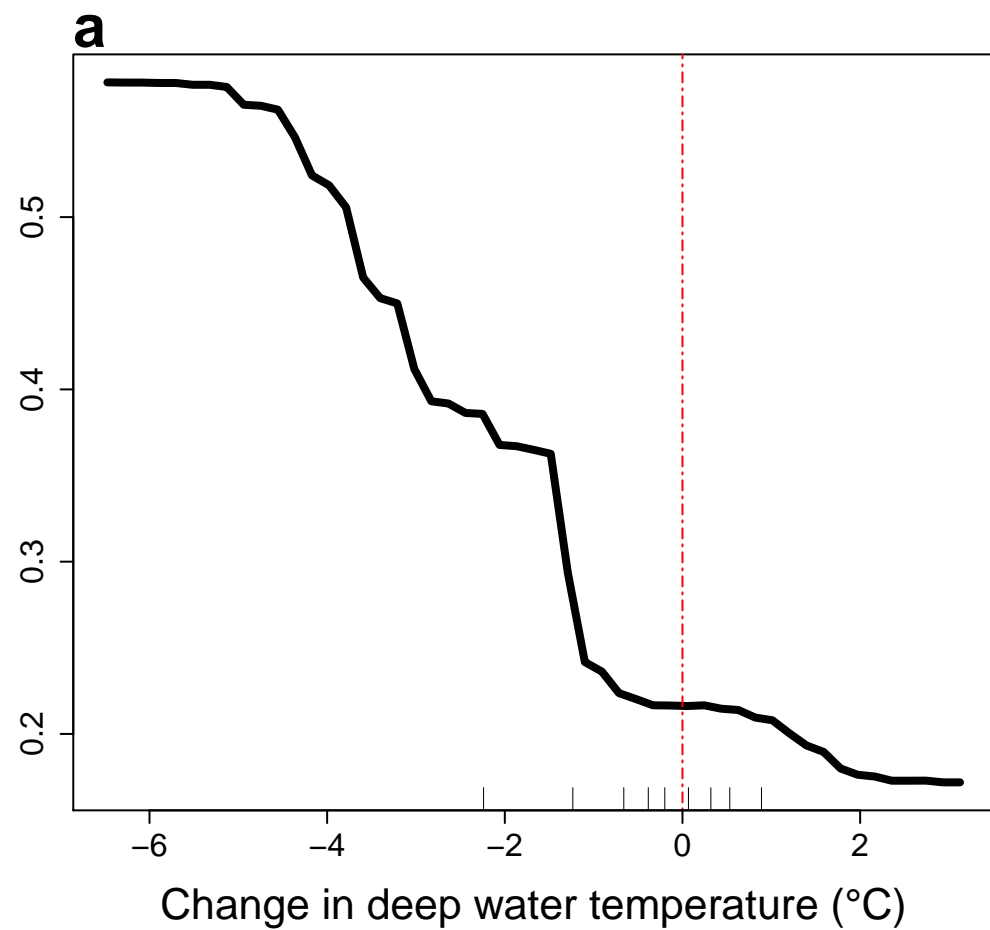


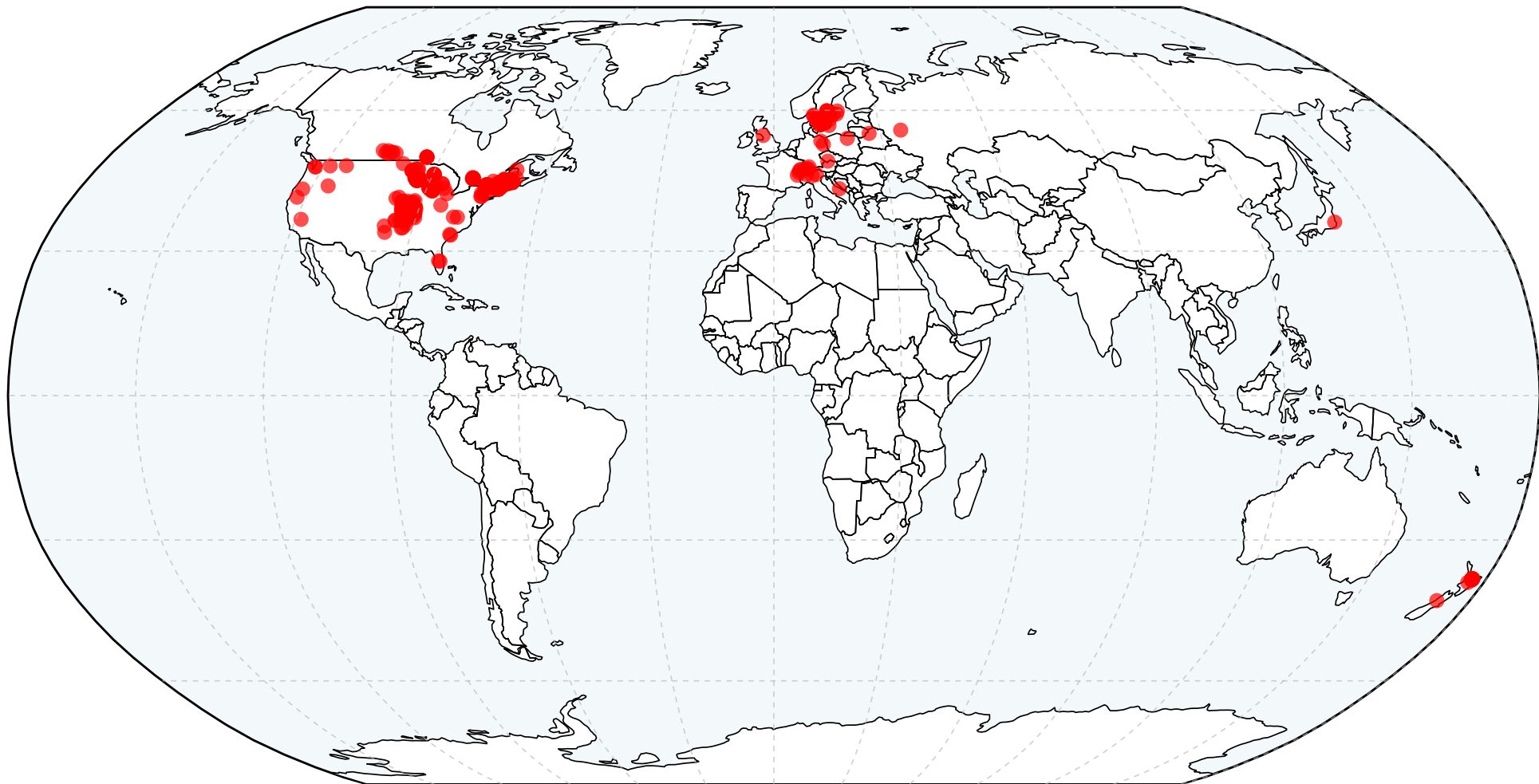
Change in percent saturation ( $\Delta$  Sat)





Change in density difference ( $\text{kg m}^{-3}$ )





## 462 **Methods:**

### 463 **Overview**

464 Our methods here describe how we 1) compiled and quality-checked data, 2) interpolated  
465 and delineated water layer strata, and 3) statistically analyzed these data. Our statistical analyses  
466 focused on characterizing long-term trends in climate characteristics (air temperature, wind  
467 speed, precipitation, and short-wave radiation), DO concentration and saturation, water  
468 temperature, and deep-water habitat quality; identifying and characterizing potential non-  
469 linearity in DO concentration and water temperature through time; characterizing the relationship  
470 between DO concentration changes and solubility, chlorophyll, and land use; identifying the  
471 predictors of changes in deep-water DO saturation, and characterizing meteorological drivers of  
472 surface temperature trends. These methods are described in detail in the sections below.

### 473 **Data compilation and quality control**

474 We compiled lake temperature and DO concentration water column measurements from a  
475 wide range of government, university, and not-for-profit sources (Fig. S4 and Tables S3 and S4).  
476 To assess long-term trends in temperature and DO concentration, we required profiles be made at  
477 least once annually during the peak summertime stratification (defined as the late summer  
478 period, July 15 - August 31 for northern hemisphere lakes and January 15 - February 28 for  
479 southern hemisphere lakes) offshore (e.g., nearest the deepest location in each lake) for at least  
480 15 years. In some larger lakes ( $n = 6$  lakes), we used profiles from two separate locations if the  
481 lake had more than one distinct basin and treated these as separate waterbodies. For some  
482 analyses other than long-term trend analyses we included lake time series data less than 15 years  
483 long, but always at least 10 years in duration (described below).

484 We conducted quality control on the compiled data as follows. We first removed  
485 impossible values, defined as those outside the range 0-40 for both temperature (units: °C) and  
486 DO concentration (units: mg L<sup>-1</sup>). We then removed profiles from consideration if our initial  
487 quality control step process removed greater than 95% of the profile or if the profile had less  
488 than three distinct depth points. To reduce the potential impacts of DO measurements made  
489 when sensors sat on or in sediments, we removed the deepest measurement for individual  
490 profiles if the maximum depth for that profile exceeded the maximum depth of 90% of the  
491 remaining profiles for a given lake.

492 Not all profiles surveyed the entire water column. Some lakes had some profiles where  
493 the shallowest depth was greater than 0 (meaning near-surface measurements were not made),  
494 yet temperature measurements showed the nearest surface measurements were within the  
495 epilimnion. In these cases, we made the assumption of uniform DO and temperature from the  
496 surface to the shallowest measurement and added a 0 m depth point. We did this by either 1)  
497 changing the minimum depth in the profile to 0 if it was less than 0.5 m, 2) adding a 0 depth  
498 point and assigning temperature and DO values equal to that of the minimum depth point if the  
499 minimum depth point was greater than or equal to 0.5 m but less than or equal to 3 m. If the  
500 minimum depth was greater than 3 m, we excluded the profile from analyses. If there were  
501 multiple values of either temperature or DO for a given depth, the mean value at this depth was  
502 used. These operations and all further analyses were conducted in R version 3.4.2<sup>29</sup>.

503 In total, the above QA steps removed 2,040 profiles out of a total of 25,023 (8.2%). After  
504 processing and removing eight non-temperate lakes, we had 22,574 DO profiles with  
505 corresponding temperature profiles. There was a median of 2.1 profiles per year (range: 1-38)  
506 and 23 years of data per lake (see also, Table S4).

## 507 **Profile interpolation and strata delineation**

508           In order to generate a dataset with consistent depth resolution within and among lakes,  
509 we interpolated each temperature and DO profile from depth 0 m to the deepest depth of each  
510 profile at intervals of 0.5 m using the `pchip` function of the R package `pracma`<sup>30</sup>. This  
511 interpolation procedure preserves the overall shape of the profile by preventing overshooting of  
512 data values<sup>30</sup>. Following interpolation, we calculated temperature and stability characteristics  
513 using the R package `rLakeAnalyzer`<sup>31</sup>. We delineated the epilimnion and hypolimnion using the  
514 `meta.depths` function (`slope = 0.1`, `seasonal = FALSE`), which calculates the top and bottom  
515 depths of the metalimnion<sup>31</sup>. If the range of temperatures through the profile is less than 1°C, the  
516 `meta.depths` function does not return values for the metalimnion (i.e., the profile is not  
517 considered stratified).

518           Many lakes did not have a well-defined hypolimnion. To identify those with a  
519 hypolimnion, we first removed lakes where the `meta.depths` function failed to calculate a bottom  
520 metalimnion depth for more than 10% of profiles. We then calculated the mean of the maximum  
521 profile depths across all profiles for each lake, to get a mean profile depth for the lake. If the  
522 mean value of the bottom of the metalimnion for a lake was shallower than the calculated mean  
523 profile depth for that lake, it was considered to have a hypolimnion. We defined “surface waters”  
524 as all depths shallower than or equal to the top metalimnetic depth and “deep waters” as all  
525 depths deeper than the bottom depth of the metalimnion.

## 526 **Characterizing trends in dissolved oxygen and temperature**

527           We calculated the mean surface- or deep-water temperature and DO concentration and  
528 percent saturation. For each lake, we calculated the mean of surface- or deep-water DO

529 concentration or temperature for all profiles in a given year (in our defined late-summer period)  
530 to obtain a mean annual value. We then calculated the percent DO saturation from temperature,  
531 DO concentration, and lake elevation data<sup>32</sup>. Mean annual surface- and deep-water temperature  
532 and DO concentration measurements were then used to calculate long-term trends for surface  
533 waters (n = 393 lakes; median number of years per lake: 24) and deep waters (n = 260; median  
534 number of years: 24). All trends were calculated using the nonparametric Sen's slope in the R  
535 package `openair`<sup>33</sup>. For trend analysis, we only used lakes with at least 15 years of data.

536         For deep-water trends, lakes that were essentially anoxic (average hypolimnetic DO < 0.5  
537 mg L<sup>-1</sup>) had trend magnitudes that clustered near 0 relative to other lakes. This was not  
538 unexpected as lakes with essentially no hypolimnetic DO have little potential to lose additional  
539 DO. When calculating median trends and for graphical depiction of trends (Fig. 1), we removed  
540 these lakes (n = 69; difference = 191).

541         We conducted several analyses to examine the potential of variability in lake data  
542 through time (i.e., not all lakes sampled all years of observation) or variability in space (i.e.,  
543 some regions sampled much more heavily than others) to influence overall population level  
544 trends (see following sections and Tables S5-S6).

### 545 **Spatial autocorrelation and effects of lake clusters**

546         Because the lakes included in this study were not uniformly dispersed over all continental  
547 land masses, we examined the potential of large numbers of lakes in relatively concentrated  
548 regions to drive overall patterns. To do this, we first examined spatial autocorrelation in trends in  
549 lake temperature and dissolved oxygen concentration using Moran's I in the R package `lctools`<sup>34</sup>.  
550 <sup>35</sup>. This statistic ranges from -1 for data that are perfectly dispersed to +1 for data that are

551 perfectly autocorrelated. Values near zero suggest randomly distributed data. We observed weak  
552 but significant spatial autocorrelation in some variables (Table S5; Moran's I values ranging 0.02  
553 to 0.27).

554 Following this analysis, we examined the potential for the large numbers of lakes in some  
555 regions to dominate overall trends we reported. We tested for potential bias by examining trends  
556 for a subset of lakes. We identified four regions in the US with high numbers of lakes (Maine =  
557 113 lakes, New Hampshire = 38 lakes, Missouri = 41 lakes, and Minnesota = 84 lakes). For each  
558 of these clustered regions, we randomly subsampled 10% of the lakes. After this random  
559 subsetting, we found that the overall trends are similar to the trends obtained from all lakes (see  
560 Table S6). These results demonstrate that our observed population-level trends are not driven  
561 solely by trends observed in our lake-rich regions. While our analysis focuses on temperate  
562 lakes, we obtained data from a small number of non-temperate lakes (n=8). Including these non-  
563 temperate lakes in our analysis (Table S6) did not change our overall results.

#### 564 **Uncertainty estimates and temporal variation in trends**

565 We conducted an analysis to compare trends, confidence intervals, and significance of  
566 trends over two time periods: 1980-2017 (n = 80) and 1990-2017 (n = 197) to assess whether  
567 different lake observation years influenced the overall trends in DO concentration and  
568 temperature we observed. For each time period, we used a subset of lakes that had data for at  
569 least 80% of years within the defined time period. Following established methods<sup>18</sup>, we  
570 calculated a yearly anomaly in temperature and dissolved oxygen for each lake as the difference  
571 between each year's observation and the long-term mean. We then averaged these anomalies  
572 across all lakes and used linear regression to calculate the slope, significance, and confidence  
573 intervals of these averaged anomalies (Table S7).

## 574 **Characterizing trends in climate characteristics**

575 We examined trends in air temperature, total precipitation, wind speed, and shortwave  
576 radiation using the ERA-5 reanalysis from the European Centre for Medium-Range Weather  
577 Forecasts (ECMWF)<sup>36</sup>. This data set provides a single gridded global product with a resolution  
578 of 0.25° latitude by 0.25° longitude over the period 1979-2019 available as monthly averages (air  
579 temperature, wind speed, and shortwave radiation) or totals (precipitation). We used ECMWF  
580 time-series data from the gridded location closest to each lake and over the two-month period  
581 around when lakes were sampled (July-August for Northern hemisphere lakes, January-February  
582 for Southern hemisphere lakes). We calculated temporal trends in mean summer air temperature,  
583 mean summer wind speed, summer total precipitation, mean summer shortwave radiation, mean  
584 winter air temperature, mean spring air temperature, mean fall air temperature using the same  
585 methods we used to examine lake temperature and DO trends (see above). We then conducted a  
586 multiple regression analysis to assess which of these predictor variables (trends in air  
587 temperature, total precipitation, wind speed, or shortwave radiation) best explained surface-water  
588 temperature trends.

## 589 **Trends in climatic variables over the temperate zone**

590 We delineated gridded latitude and longitudes at 2° intervals across the entire temperate  
591 zone over land masses only as well as over large regions, including Asia (defined by longitude  $\geq$   
592 29.3°; latitude 23.5° to 60°) Europe and North America (longitude  $<$  29.3°; latitude 23.5° to 60°),  
593 South America and western Africa (longitude  $<$  0°; latitude  $\leq$  -23.5° to -60°); and southern  
594 Africa, Australia, and Oceania (longitude  $\geq$  0°; latitude -23.5° to -60°). We then used data from  
595 the ERA-5 reanalysis (see ‘Characterizing trends in climate characteristics’ in Methods for  
596 details) to calculate trends in climate variables over each of these regions (Table S1).



## 597 **Multiple regression analysis of drivers of surface water temperature trends**

598 We conducted a multiple regression analysis of the meteorological drivers of observed  
599 surface water temperature trends. Predictors in the analysis included: summer air temperature  
600 trend, summer total precipitation trend, summer wind speed trend, summer shortwave radiation  
601 trend, winter air temperature trend, spring air temperature trend, fall air temperature trend, and  
602 mean winter temperature (as a proxy for ice cover<sup>18</sup>). We z-score standardized all variables to  
603 facilitate comparison of model coefficients across variables having different units<sup>37</sup>. We verified  
604 that multicollinearity was not a problem by checking that the variance inflation factor was well  
605 below ten for all variables<sup>38</sup>. We used the leaps R package to select subset models including all  
606 predictors and two-way interactions, and selected the fitted model having the lowest AIC<sup>39</sup>.  
607 Coefficients and p-values for the selected model appear in Table S2.

## 608 **Characterizing trends in deep-water habitat quality**

609 We used  $T_{\text{DO3}}^{\text{11}}$  to quantify trends in oxythermal habitat relevant for cold-water  
610 organisms.  $T_{\text{DO3}}$  represents the minimum temperature in the water column where DO  
611 concentration was greater than or equal to 3 mg L<sup>-1</sup> and has been used to describe habitat  
612 availability for cold-water fisheries<sup>11</sup>. To calculate trends in  $T_{\text{DO3}}$  we excluded lakes where the  
613 DO concentration was higher than 3 mg L<sup>-1</sup> across all depths in all profiles. For the remaining  
614 lakes, we calculated  $T_{\text{DO3}}$  for each profile. If a given profile did not have DO below 3 mg L<sup>-1</sup>, we  
615 assigned it the minimum temperature in the profile. We then calculated an annual mean  $T_{\text{DO3}}$  for  
616 the late summer period and excluded lakes that had  $\leq 15$  years of data. This left 369 lakes where  
617 DO went below 3 mg L<sup>-1</sup> at least once.

## 618 **Non-linearity in DO and temperature through time**

619 We conducted a generalized additive mixed model (GAMM) analysis to characterize  
620 overall response of lake temperature and DO concentration through time and to identify any non-  
621 linearity. GAMMs fit a smooth function of the predictor variables showing the relationship of the  
622 predictors to the response variable<sup>40</sup>. We conducted separate analyses for four response variables,  
623 surface-water temperature, surface-water DO concentration, deep-water temperature, and deep-  
624 water DO concentration. For each GAMM, our only predictor variable was the year, resulting in  
625 models that show the change in the response variable through time. We used the gamm4 function  
626 of the gamm4 package to fit these models using the default thin plate spline for smooth terms<sup>41</sup>.  
627 Gamm4 uses penalized regression splines of moderate rank for the smooth function. For two of  
628 these models we used a normal error distribution. Because residuals for the deep-water  
629 temperature analysis were skewed, we used a gamma distribution. Residuals in the deep-water  
630 DO analysis were also skewed, but because there were a large number of 0 values we used a  
631 Tweedie distribution instead of a gamma distribution. We limited this analysis to data from 1970  
632 and later and included all lakes with data in the specified time period (total lake n = 419). To  
633 account for the non-independent nature of the repeated measurements through time within each  
634 individual lake, the slope and intercept were allowed to vary randomly by lake<sup>42</sup>.

635 We next conducted a GAMM to understand how surface water DO concentration  
636 responded to temperature and productivity (n = 419 lakes). We used Secchi disk depth as a  
637 surrogate for productivity<sup>19</sup>. We included fixed effects of mean summer surface water  
638 temperature, mean Secchi depth, and the interaction of these two terms in the model. We  
639 included a random intercept and slope by year within each lake and included a corresponding  
640 year fixed effect.

641 **Relationship between dissolved oxygen concentration changes and solubility**

642 To determine the relative importance of solubility in explaining changes in DO  
643 concentration, we calculated the expected change in DO concentration due to solubility alone  
644 and compared this amount to the observed DO change. To do this, we first calculated the  
645 difference between the observed mean DO concentration across the last five years and the first  
646 five years of record for each lake, requiring a minimum of ten years of data per lake (n = 415  
647 lakes for surface (Fig. 2a); n = 259 lakes for deep (Fig 2b)). We then calculated the expected  
648 change due solely to solubility and compared observed to expected DO changes. Specifically, we  
649 calculated the mean percent saturation in the first five years by first calculating the mean DO  
650 saturation for each water column layer (surface or deep waters) and then calculated the mean of  
651 all of these values. We then used an analogous approach to calculate mean temperature, DO  
652 concentration, and mean DO concentration at 100% saturation in the last five years of record for  
653 each lake. Once we calculated these values, we multiplied the mean DO concentration at 100%  
654 saturation by the decimal value of percent saturation in the first five years of record. This product  
655 represents the expected DO concentration if the percent saturation in the last five years of record  
656 remained the same as it was in the first five years of record. In other words, we removed the  
657 effect of temperature so that if all changes were due solely to solubility, observed changes in DO  
658 concentration would be identical to this value.

### 659 **Relationship between dissolved oxygen trends and chlorophyll**

660 We used multiple regression to test if chlorophyll concentration and surface-water  
661 temperature were predictors of lakes having both increasing surface DO concentration and  
662 temperature trends. We first calculated the long-term mean late-summer surface-water  
663 (epilimnetic) chlorophyll concentration, which was available for 162 lakes having at least ten  
664 years of chlorophyll measurements. We next predicted DO concentration trends using

665 chlorophyll and mean surface-water temperature as independent variables. We first fit the linear  
666 regression models, starting with a full model that included the interaction of chlorophyll and  
667 temperature. We then fit all subset models and selected the model with the lowest AIC value<sup>43</sup>.  
668 Using this selected model, we predicted DO concentration trends at three different mean  
669 epilimnetic temperatures (21, 25, and 28°C) across the observed values for chlorophyll.

## 670 **Relationship between dissolved oxygen trends and land use**

671 We used logistic regression to better understand the drivers of increasing DO  
672 concentration in lakes with increasing surface-water temperatures, using land use/land cover data  
673 to model the probability of this phenomenon<sup>44</sup>. Logistic regression predicts the probability of a  
674 binary response outcome for different values of predictor variables. Predictors in our logistic  
675 regression included the percent of agriculture and developed land cover in the watershed and the  
676 mean surface-water temperature over the last ten years of record because these land use  
677 characteristics have been associated with increased growth of some phytoplankton taxa in  
678 warmer lakes<sup>5,21</sup>. Our binary response was: either a lake had both increasing surface temperature  
679 and DO concentration (1) or it did not (0). We tested for all two-way interactions and all main  
680 effects. We used the National Land Cover Database 2011 to derive land cover metrics for US  
681 lakes<sup>45</sup>. We considered any land falling into any of the developed classes as developed  
682 (Developed – Open Space, Developed – Low Intensity, Developed – Medium Intensity,  
683 Developed – High Intensity). We tested the goodness of fit of the final model using the Hosmer-  
684 Lemeshow test, available in the ResourceSelection R package (function `hoslem.test`)<sup>46</sup>. This test  
685 showed an acceptable goodness of fit ( $P = 0.166$ ). The final number of lakes for analysis that had  
686 both land cover data and sufficient data to calculate trends was 326.

## 687 **Identifying the predictors of changes in deep-water DO saturation**

688           We first used a random forest algorithm to obtain predictors of the observed change in  
689 percent saturation (i.e., drivers beyond pure solubility effects) in deep waters<sup>47</sup>. We used the  
690 percent increase in mean squared error as a measure of predictor variable importance. We  
691 conducted the random forest algorithm analysis using the randomForest package<sup>48</sup>. For each  
692 analysis, we only used lakes that had no missing values for any of the predictor variables (n =  
693 224 lakes).

694           For the random forest algorithm, the response variable was the change in mean DO  
695 percent saturation in the last five years of record relative to the first five years of record for each  
696 lake ( $\Delta$  Sat). A positive  $\Delta$  Sat indicated an increase in percent saturation while a negative  $\Delta$  Sat  
697 indicated a decrease in percent saturation. Predictor variables included mean hypolimnetic DO  
698 percent saturation, DO concentration, temperature, and thickness of the hypolimnion (ln  
699 transformed), mean Secchi depth, ln of mean lake depth, log10 of residence time, change in  
700 hypolimnetic thickness, change in hypolimnetic temperature, change in Secchi depth, and change  
701 in the density difference between surface and deep waters. Mean lake depth and residence time  
702 were obtained from the HydroLakes Database<sup>49</sup>. We calculated the density difference across the  
703 water column using rLakeAnalyzer to calculate densities for each interpolated depth point in  
704 each water column profile<sup>31</sup>. If a given profile was stratified, we then used the mean epilimnetic  
705 density and the mean hypolimnetic density and calculated the difference between these densities.  
706 If a given profile was not stratified, we took the mean density across the top two meters and the  
707 mean density across the bottom two meters and calculated the difference between these densities.  
708 We also included trends in the following ERA-5 meteorological variables: summer, fall, and  
709 winter air temperature, summer shortwave radiation, and summer wind speed. Finally we  
710 included mean winter air temperature as a proxy for ice cover<sup>18</sup>.

711           Following the above analysis, change in the density difference between surface and deep  
712 waters came out as an important predictor. Although this could be explained by increased surface  
713 water temperatures driven by meteorological variables, it is possible that other changes, such as  
714 water clarity<sup>25</sup>, could also explain changes in density difference. To disentangle the drivers of  
715 changes in water column density differences, we conducted another RF using the same predictor  
716 variables as the above analysis but changing the response variable to the change in the density  
717 difference. We did not include the response variable from the first analysis ( $\Delta$  Sat). The six most  
718 important variables are presented in Fig. S3.

719           Based on results of the RF analysis, we conducted a multiple regression analysis to  
720 predict change in percent saturation ( $\Delta$  Sat) for different levels of predictor variables (ln of mean  
721 lake depth, change in the density difference across the water column, and change in Secchi  
722 depth). We used a subset of lakes where mean deep-water DO concentration exceeded 0.5 mg/L  
723 to avoid lakes with little potential to lose DO. Predictor variables were selected because they  
724 were the three most important variables identified by RF, except we substituted ln mean lake  
725 depth for ln deep layer thickness. This substitution was made because models using ln of deep  
726 layer thickness demonstrated substantial non-linearity in plots of residuals against fitted values.  
727 Models built with ln mean lake depth greatly improved these patterns and these two variables  
728 were correlated ( $r = 0.51$ ). We first fit the multiple regression models starting with a full model  
729 that included all predictors and two-way interaction terms. We then fit all subset models and  
730 selected the model with the lowest AIC value<sup>43</sup>. Using this selected model, we predicted  $\Delta$  Sat at  
731 three different values of each of the two predictors change in Secchi depth ( $P < 0.001$ ) and  
732 change in water column density difference ( $P < 0.001$ ), with ln mean lake depth held at the  
733 median value.

734

735 **Data Availability:**

736 Many of the datasets analyzed during this study are publicly available on-line and associated  
737 links can be found in supplementary Table S3. Derived statistics are publicly available via the  
738 Environmental Data Initiative (EDI) repository at  
739 <https://doi.org/10.6073/pasta/ac8b05bb0da19032b3df3efc21f83874>. Most lakes are included  
740 here, but we note that due to the collaborative nature of this project and a wide range of data  
741 provenance, it was not possible to include every lake in this repository. Data not otherwise  
742 already publicly available are available upon request from the corresponding author pending  
743 permission from the appropriate data provider.

744

745 **References:**

- 746 29. R Core Team. R: a language and environment for statistical computing. R foundation for  
747 statistical computing, Vienna, Austria (2017).
- 748 30. Borchers, H. W. pracma: Practical Numerical Math Functions. R package version 2.1.5  
749 <https://CRAN.R-project.org/package=pracma> (2018).
- 750 31. Winslow, L. A., et al. rLakeAnalyzer: Lake Physics Tools. R package version 1.11.4.  
751 <https://CRAN.R-project.org/package=rLakeAnalyzer> (2017).
- 752 32. Winslow, L. A., et al. LakeMetabolizer: An R package for estimating lake metabolism from  
753 free-water oxygen using diverse statistical models. *Inland Waters*, **6**, 622-636 (2016).
- 754 33. Carslaw, D. C., & Ropkins, K. Openair – An R package for air quality data analysis. *Environ.*  
755 *Model. Softw.*, 27-28, 52-61 (2012).

- 756 34. Moran, P. A. P. The interpretation of statistical maps. *J. Roy. Stat. Soc. B Met.*, **10**, 243-251  
757 (1948).
- 758 35. Kalogirou, S. lctools: Local Correlation, Spatial Inequalities, Geographically Weighted  
759 Regression and Other Tools. R package version 0.2-7. [https://CRAN.R-](https://CRAN.R-project.org/package=lctools)  
760 [project.org/package=lctools](https://CRAN.R-project.org/package=lctools) (2019).
- 761 36. Copernicus Climate Change Service (C3S). ERA5: Fifth generation of ECMWF atmospheric  
762 reanalyses of the global climate. Copernicus Climate Change Service Climate Data Store  
763 (CDS), Accessed 10/1/2019. <https://cds.climate.copernicus.eu/cdsapp#!/home>
- 764 37. Gelman, G., & Hill, J. *Data Analysis Using Regression and Multilevel/Hierarchical Models*.  
765 Cambridge University Press, New York (2007).
- 766 38. Quinn, G. P., & Keough, M. J. *Experimental Design and Data Analysis for Biologists*.  
767 Cambridge University Press, Cambridge, U. K. (2002).
- 768 39. Lumley, T. leaps: Regression Subset Selection (based on Fortran code by Alan Miller). R  
769 package version 3.1. <https://CRAN.R-project.org/package=leaps> (2020).
- 770 40. Wood, S. N. *Generalized Additive Models: An Introduction with R* (2<sup>nd</sup> edition). CRC Press.  
771 Boca Raton, FL (2017).
- 772 41. Wood, S., & Scheipl, F. gamm4: Generalized Additive Mixed Models using ‘mgcv’ and  
773 ‘lme4’. R package version 0.2-5. <https://CRAN.R-project.org/package=gamm4> (2017).
- 774 42. Pinheiro, J. C., & Bates, D. M. *Mixed Effects Models in S and S-Plus*. Springer, New York  
775 (2000).



- 776 43. Burnham, K. P., Anderson, D. R., & Huyvaert, K. P. AIC model selection and multimodel  
777 inference in behavioral ecology: some background, observations, and comparisons. *Behav.*  
778 *Ecol. Sociobiol.*, **65**, 23-35 (2011).
- 779 44. Hosmer, D. W., & Lemeshow, S. *Applied Logistic Regression* (2<sup>nd</sup> edition). John Wiley and  
780 Sons, Inc., New York (2000).
- 781 45. Homer, C. G., et al. Completion of the 2011 National Land Cover Database for the  
782 conterminous United States – Representing a decade of land cover change information.  
783 *Photogramm. Eng. Remote Sensing*, **81**, 345-354 (2015).
- 784 46. Lele, S. R., Keim, J. L., & Solymos, P. ResourceSelection: Resource Selection (Probability)  
785 Functions for Use-Availability Data. R package version 0.3-2. [https://CRAN.R-](https://CRAN.R-project.org/package=ResourceSelection)  
786 [project.org/package=ResourceSelection](https://CRAN.R-project.org/package=ResourceSelection) (2017).
- 787 47. Cutler, D. R., et al. Random forests for classification in ecology. *Ecology*, **88**, 2783-2792,  
788 (2007).
- 789 48. Liaw, A., & Wiener, M. Classification and regression by randomForest. *R News*, **2**, 18-22  
790 (2002).
- 791 49. Messenger, M. L., Lehner, B., Grill, G., Nedeva, I., & Schmitt, O. Estimating the volume and  
792 age of water stored in global lakes using a geo-statistical approach. *Nat. Commun.*, **7**, 13603,  
793 doi:10.1038/ncomms1360 (2016).
- 794